Magnetic scaling in cuprate superconductors

V. Barzykin and D. Pines
Department of Physics and Science and Technology Center for Superconductivity, University of Illinois at Urbana-Champaign, Urbana, Illinois 61801-3080
(Received 2 March 1995)

We determine the magnetic phase diagram for the $YBa_2Cu_3O_{6+x}$ and $La_{2-x}Sr_xCuO_4$ systems from various NMR experiments. We discuss the possible interpretation of NMR and neutron scattering experiments in these systems in terms of both the nonlinear σ model of nearly localized spins and a nearly antiferromagnetic Fermi liquid description of magnetically coupled quasiparticles. We show for both the 2:1:4 and 1:2:3 systems that bulk properties, such as the spin susceptibiltiy, and probes at the antiferromagnetic wave vector (π,π), such as $^{63}T_1$, the ^{63}Cu spin-lattice relaxation time, both display a crossover at a temperature T_{cr}, which increases linearly with decreasing hole concentration, from a nonuniversal regime to a $z=1$ scaling regime characterized by spin pseudogap behavior. We pursue the consequences of the ansatz that T_{cr} corresponds to a fixed value of the antiferromagnetic correlation length ξ and show how this enables one to extract the magnitude and temperature dependence of ξ from measurements of T_1 alone. We show that like T_{cr}, the temperature T_* which marks a crossover at low temperatures from the $z=1$ scaling regime to a quantum disordered regime, exhibits the same dependence on doping for the 2:1:4 and 1:2:3 systems, and so arrive at a unified description of magnetic behavior in the cuprates, in which the determining factor is the planar hole concentration.

I. INTRODUCTION

The exotic magnetic properties of high-temperature superconductors have been extensively studied during the last few years, both because of their intrinsic interest and in the hope that these might provide insight in the physical origin of high-temperature superconductivity. Although considerable progress has been made in understanding the magnetic behavior of these materials, the basic issues of the doping dependence of the magnetic phase diagram and the relationship between transport properties and magnetic behavior in the normal state of the superconducting cuprates have not yet been completely resolved. In this paper we construct new magnetic phase diagrams for the $YBa_2Cu_3O_{6+x}$ and $La_{2-x}Sr_xCuO_4$ system on the basis of NMR experiments.[1] Our approach makes evident the connection between the appearance of a spin pseudogap and magnetic scaling, and enables us to deduce from NMR experiments of the ^{63}Cu spin-lattice relaxation rate the magnitude and temperature dependence of the length, ξ, which characterizes the strength of the antiferromagnetic correlations found in both underdoped and fully doped cuprate superconductors.

It is well established that the undoped materials are described by the two-dimensional (2D) Heisenberg model with a fairly large exchange coupling $J\simeq 1550$ K.[2] The thermal fluctuations destroy long-range order at finite temperature (the Hohenberg-Mermin-Wagner theorem), and the Néel transition observed in undoped cuprates is solely due to the small, but finite interplanar coupling. Chakravarty *et al.*[3] gave a strong indication that the long-wavelength action of $s=1/2$ 2D Heisenberg antiferromagnet is reduced to the quantum nonlinear σ model, characterized by an action,

$$S_{\rm eff}=\frac{\rho_S^0}{2}\int_0^{\beta\hbar} d\tau \int d^2x\left[(\nabla \mathbf{n})^2+\frac{1}{c_0^2}(\partial_\tau \mathbf{n})^2\right]. \quad (1)$$

Here $\mathbf{n}$ is a three-component vector field, which describes the local staggered magnetization, which is subject to the constraint $|\mathbf{n}|=1$, ρ_S^0 is the spin stiffness, and c_0 is the spin wave velocity. There is a short-distance cutoff Λ^{-1} for the spatial integrals. The properties of the σ model are conveniently expressed in terms of the coupling constant $g=\hbar c_0/\rho_S^0$. Chakravarty *et al.*[3] identified three different regimes of behavior (Fig. 1), defined by the zero-temperature ordered-nonordered phase transition at $g_c=4\pi/\Lambda$. According to the σ-model g-T phase diagram, for all coupling constants there exists a high-temperature quantum critical (QC) regime $[(\rho_S,\Delta)\lesssim T\lesssim J]$ in which the characteristic energy scale is set by temperature. At lower temperatures, depending on the coupling constant g, the correlation length either grows exponentially, as in the renormalized classical (RC) regime (for $g<g_c$), or stays constant, as in the quantum disordered (QD) regime (for $g>g_c$). For the states without long-range order ($g>g_c$ or $T>0$) the Goldstone mode is eliminated, which leads to a finite gap in the spin-wave spectrum $\Delta=c/\xi$, where c is the spin-wave velocity and ξ the correlation length.

Doping changes the ground state of the cuprates from a Neél-ordered state to a highly correlated ground state without long-range order.[4] It was first argued by Sachdev and Ye[5] that the behavior of the cuprates for small doping is controlled by the zero-temperature critical point of the σ model leading to the dynamic critical exponent $z=1$. This critical point does not necessarily correspond to the metal-insulator transition. The quantum critical $z=1$ transition exhibited by the σ model was then analyzed in detail by Chubukov *et al.*,[6] who emphasized its potential importance for the magnetic phase diagram of the cuprate superconductors.

On the basis of NMR experiments of Imai *et al.*[7] and Takigawa,[8] Sokol and Pines[9] then argued that the σ model,

 © 1995 The American Physical Society

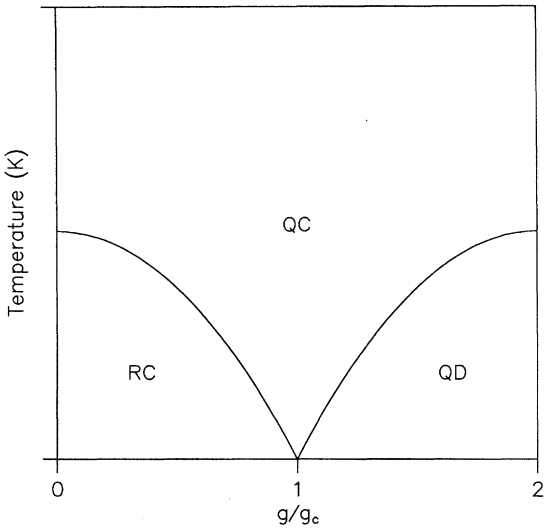

FIG. 1. The phase diagram of the σ model from Chakravarty *et al.* (Ref. 3).

QC $z=1$, description of the spin fluctuations continues to be valid at the comparatively large doping levels which are appropriate to the underdoped cuprate superconductors. They suggested that a spin wave description is valid at high temperatures for these systems, while at higher doping levels, such as are found in $YBa_2Cu_3O_7$, the particle-hole excitations act to completely damp the spin wave spectrum, so that the normal state of $YBa_2Cu_3O_7$ is best described using the nearly antiferromagnetic Fermi liquid (NAFL) model which had been successfully applied to the analysis of NMR experiments in both its normal and superconducting states.[10–12] In this mean-field model the spin fluctuations at (π,π) are characterized by a relaxational mode which varies as ξ^{-2}; thus it resembles a system with the dynamical critical exponent $z=2$. In Ref. 13 the mean-field formula for the crossover from $z=1$ to $z=2$ was obtained by incorporating the quasiparticle damping in the σ-model expression for the spin susceptibility, and different experiments were analyzed using this formula. A major step towards the description of the $z=1$ to $z=2$ crossover has been taken recently by Sachdev *et al.*,[14] who explicitly derive the crossover scaling functions of the spin-fermion model using a $1/N$ expansion.

A very general analysis of both NAFL and nearly ferromagnetic Fermi liquid behavior has been carried out by Millis[15] and Altshuler *et al.*[16] while Monthoux and Pines[17] (MP), have discussed the possibility that a NAFL approach, in which non-linear feedback from the magnetic interaction between quasiparticles acts to bring about a spin pseudogap in the quasiparticle spectrum, might yield the functional equivalent of QC $z=1$ behavior over a broad temperature region in the underdoped cuprates, with overdamped spin waves arising because the magnetic energy, $\omega_J \sim$ a few J, and the quasiparticle Fermi energy are on approximately the same scale. They suggested that the onset of the pseudogap would occur at a certain value of the correlation length, which is independent of doping.

In the present paper we extend previous analyses of NMR experiments[9,13] on the metallic low-temperature normal state regimes of $La_{2-x}Sr_xCuO_4$ and $YBa_2Cu_3O_{6+x}$ systems and

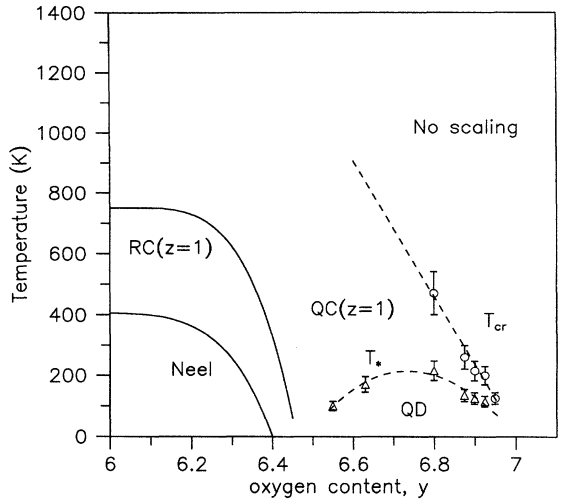

FIG. 2. The magnetic phase diagram determined from NMR experiments on the $YBa_2Cu_3O_{6+y}$ system. The temperature T_{cr} marks the crossover from nonuniversal behavior to spin pseudogap behavior, while T_* marks the crossover from QC $(z=1)$ scaling behavior to QD behavior. Scaling behavior is thus found between T_* and T_{cr}.

present revised magnetic phase diagrams (Fig. 2 and Fig. 3) which make explicit the presence of both an upper limit T_{cr} and a lower limit T_* to QC $z=1$ scaling behavior in these systems. We show that T_{cr} both marks the onset of spin pseudogap behavior, a reduction of the effective quasiparticle density of states, found first in bulk susceptibility[18] and Knight shift[19] experiments, and subsequently in specific heat experiments,[20] and the crossover from a high-temperature nonuniversal regime to a low-temperature universal scaling regime. This scaling regime has dynamical critical exponent $z=1$. We argue that this crossover happens at a fixed value

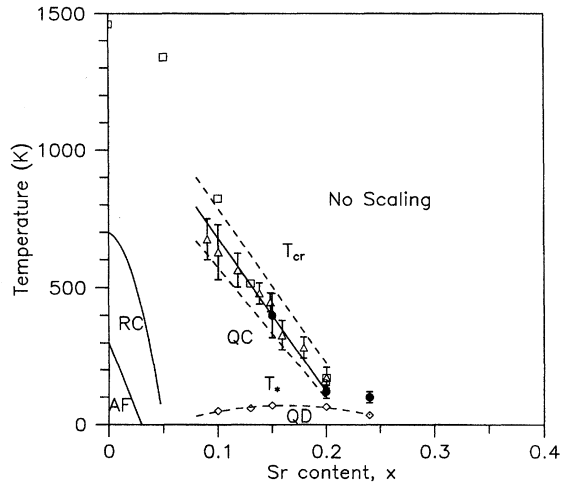

FIG. 3. The magnetic phase diagram determined from NMR and bulk susceptibility experiments on the $La_{2-x}Sr_xCuO_4$ system. The solid circles represent values of T_{cr} determined by us from NMR experiments; the triangles correspond to the maximum in the bulk susceptibility reported by Hwang *et al.* (Ref. 23); the open squares are the corresponding results obtained by Johnston (Ref. 18).

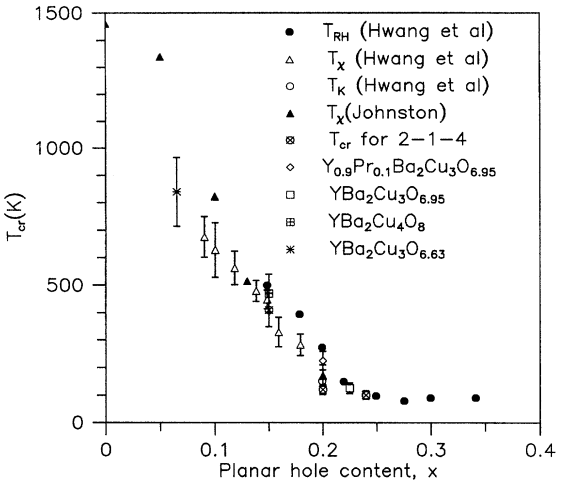

FIG. 4. The dependence on hole concentration of the temperature T_{cr} for the onset of spin pseudogap behavior determined here for the 2:1:4 and 1:2:3 systems is compared to the characteristic temperatures determined by Hwang *et al.* (Ref. 23) from transport and bulk susceptibility measurements and the maximum in bulk susceptibility found by Johnston (Ref. 18).

of the correlation length, $\xi_{cr} \simeq 2$, and that T_{cr} is close to T_χ, the temperature which marks the maximum of the spin susceptibility. We use the results of NMR experiments to determine the region of applicability of scaling and find that T_{cr} varies nearly linearly with doping level over a region which extends from the AF insulators $YBa_2Cu_3O_6$ and La_2CuO_4 to $YBa_2Cu_3O_7$ and the overdoped system $La_{1.76}Sr_{0.24}CuO_4$. We find (see Fig. 4) that when the crossover temperature T_{cr} is plotted as a function of planar hole doping, within experimental uncertainties, one finds the same dependence on doping for the 1:2:3 and 2:1:4 families. This demonstrates that the onset of magnetic scaling is determined only by hole concentration (band-structure effects are unimportant) and that bilayer coupling plays little or no role in determining spin pseudogap and scaling behavior.

The QC-QD crossover at T_*, which is predicted by the σ model at lower temperatures, is also identified from the NMR data. Our identification of the experimentally determined "spin pseudogap" temperature T_{cr} with a fixed value of ξ then allows us to use NMR measurements of the ^{63}Cu spin-lattice relaxation rate to determine the correlation length and other parameters which characterize low-frequency magnetic behavior as a function of temperature for both the $YBa_2Cu_3O_{6+x}$ and $La_{2-x}Sr_xCuO_4$ families. We establish thereby the details of the variation with doping of the correlation length.

There exists as well an intimate relationship between spin and charge response of the underdoped cuprate superconductors. Ito *et al.*[21] showed for $YBa_2Cu_3O_{6.63}$ that below a temperature T_ρ, the planar resistivity ceases to exhibit a linear in T behavior, while the Hall effect likewise changes character at this temperature; a similar conclusion for $YBa_2Cu_4O_8$ was reached by Bucher *et al.*[22] We find that within experimental error, $T_\rho = T_*$. In the $La_{2-x}Sr_xCuO_4$ system Hwang *et al.*[23] have shown that for $x \geq 0.15$, the Hall coefficient $R_H(T)$, follows scaling behavior, with a characteristic temperature T_H, which not only exhibits the same strong dependence on doping level that is found for T_{cr}, but which possesses very nearly the same magnitude as the T_χ determined from the maximum in the spin susceptibility. For this same system, with $x \leq 0.14$, Nakano *et al.*[24] find that below T_χ, the resistivity ceases to be linear in T. Thus both the lower crossover temperature T_* and the upper crossover temperature T_{cr}, which mark the limits of the QC $z=1$ scaling behavior we identify in low-frequency magnetic measurements, possess counterparts in transport measurements.

Although there is indirect experimental evidence for their existence from NMR experiments, propagating spin waves for the underdoped cuprates have not been observed in neutron-scattering experiments on the normal state. We show, on the basis of the parameters we infer from NMR experiments, that just such a result is to be expected — that spin waves are substantially overdamped by quasiparticle interactions in the normal state. Since this damping is markedly reduced in the superconducting state, we conclude that spin-wave excitations should become visible in the superconducting state, and we present arguments which suggest that this provides a quantitative explanation for the recent experiments of Fong *et al.*[25] on inelastic neutron scattering from $YBa_2Cu_3O_7$.

Our paper is organized as follows. In Sec. II we review the one-component approach to the interpretation of NMR measurements. In Sec. III we use this to analyze the current experimental situation for the magnetic measurements in the underdoped $YBa_2Cu_3O_{6+x}$ and $La_{2-x}Sr_xCuO_4$ families, and on the basis of this analysis we arrive at our new magnetic phase diagram for these systems. In Sec. IV we discuss possible theoretical models, and the form for the spin susceptibility at high-energy transfer. We discuss the application of the scaling analysis to inelastic neutron-scattering experiments in Sec. V, and in Sec. VI we present our conclusions.

II. ONE-COMPONENT APPROACH TO NMR EXPERIMENTS

We start by giving a brief overview of the NMR experiments and their interpretation in one-component nearly antiferromagnetic Fermi liquid (NAFL) theory. The interested reader will find a more detailed discussion in the excellent recent review of NMR measurements in the cuprate superconductors by Slichter.[1]

Nuclear spins probe the local environment. The Knight shift provides a measure of the uniform magnetic susceptibility at a particular nuclear site, while the measurements of the spin-lattice relaxation rates yield information on the imaginary and real parts of the dynamic spin susceptibility $\chi(\mathbf{q},\omega)$. The single-component description of the NMR experiments in $YBa_2Cu_3O_7$ has its basic justification in the observation by Alloul *et al.*[19] and Takigawa *et al.*[26] that the ^{63}Cu, ^{17}O, and ^{89}Y Knight shifts see the same spin susceptibility. Since the ^{63}Cu spin-lattice relaxation time both has anomalous temperature dependence and is much shorter than that for the ^{17}O and ^{89}Y nuclei, it was proposed[27] that the single magnetic component formed by the system of planar Cu^{2+} spins and holes mainly resides on the planar copper sites. The Shastry-Mila-Rice (SMR) Hamiltonian,[27] which describes the coupling of the Cu^{2+} spins to the various nu-

clei in $YBa_2Cu_3O_7$, has the form

$$H_{\rm MRS}={}^{63}I_\alpha(\mathbf{r}_i)\left[\sum_\beta A^{\alpha\beta}S_\beta(\mathbf{r}_i)+B\sum_j^{nn} S_\alpha(\mathbf{r}_j)\right] + {}^{17}I_\alpha(\mathbf{r}_i)C^{\alpha\beta}\sum_{j\beta}^{nn} S_\beta(\mathbf{r}_j)+{}^{89}I_\alpha(\mathbf{r}_i)D\sum_j^{nn} S_\alpha(\mathbf{r}_j), \tag{2}$$

where $A_{\alpha\beta}$ is the tensor for the direct, on-site coupling of the ^{63}Cu nuclei to the Cu^{2+} spins and B is the strength of the transferred hyperfine coupling of the ^{63}Cu nuclear spin to the four nearest neighbor copper spins, while ^{17}O and ^{89}Y nuclei see only their nearest neighbor Cu^{2+} spins through the transferred hyperfine interactions $C^{\alpha\beta}$ and D. It follows from this Hamiltonian that different nuclei probe different regions in momentum space of $\chi(\mathbf{q},\omega\to 0)$. Using Eq. (2), it is straightforward to express the spin contribution to the Knight shifts for the various nuclei:[10]

$$ {}^{63}K_\parallel^S=\frac{(A_\parallel+4B)\chi_0}{{}^{63}\gamma_n\gamma_e\hbar^2}, \quad {}^{63}K_\perp^S=\frac{(A_\perp+4B)\chi_0}{{}^{63}\gamma_n\gamma_e\hbar^2}, $$

$$ {}^{17}K_\beta^S=\frac{2C_\beta\chi_0}{{}^{17}\gamma_n\gamma_e\hbar^2}, \quad {}^{89}K^S=\frac{8D\chi_0}{{}^{89}\gamma_n\gamma_e\hbar^2}. \tag{3}$$

Here the γ_n are various nuclei gyromagnetic ratios, γ_e is the electron gyromagnetic ratio, and χ_0 is the temperature-dependent static spin susceptibility, while the indices $\parallel$ and $\perp$ for copper nuclei refer to the direction of the applied static magnetic field with respect to the axis perpendicular to the Cu-O planes. The index β for the oxygen nuclei can be either $\parallel$ or $\perp$. The spin-lattice relaxation time $({}^\alpha T_1)_\beta$, for a nucleus α responding to a magnetic field in the β direction, is

$$ {}^\alpha T_{1\beta}^{-1}(T)=\frac{k_BT}{2\mu_B^2\hbar^2\omega}\sum_q {}^\alpha F_\beta(\mathbf{q})\chi''(\mathbf{q},\omega\to 0), \tag{4}$$

where the form factors ${}^\alpha F_\beta(\mathbf{q})$ are given by

$$ {}^{63}F_\parallel=\{A_\perp+2B[\cos(q_xa)+cos(q_ya)]\}^2, $$

$$ {}^{63}F_\perp=\tfrac{1}{2}[{}^{63}F_\parallel+{}^{63}F_{\rm eff}], $$

$$ {}^{63}F_{\rm eff}=\{A_\parallel+2B[\cos(q_xa)+\cos(q_ya)]\}^2, $$

$$ {}^{17}F_\beta=2C_\beta^2[1+\tfrac{1}{2}[\cos(q_xa)+\cos(q_ya)], $$

$$ {}^{89}F_{ISO}=16D^2\cos^2(q_za/2)[1+\cos(q_xa)][1+\cos(q_ya)]. \tag{5}$$

The form factor ${}^{63}F_{\rm eff}$ is the filter for the ^{63}Cu spin-echo decay time ${}^{63}T_{2G}$ (Ref. 28):

$$ {}^{63}T_{2G}^{-2}(T)=\left(\frac{0.69}{128}\right)^{1/2}({}^{63}\gamma_n)^2\left\{\frac{1}{N}\sum_{\mathbf{q}} F_{\rm eff}(\mathbf{q})^2[\chi'(\mathbf{q})]^2 - \left[\frac{1}{N}\sum_{\mathbf{q}} F_{\rm eff}(\mathbf{q})\chi'(\mathbf{q})\right]^2\right\}. \tag{6}$$

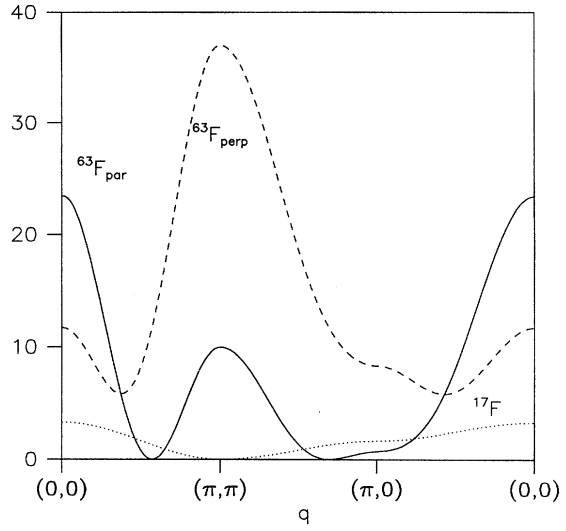

FIG. 5. Form factors as a function of momentum, for planar oxygen and copper sites, in units of the hyperfine coupling constant B^2.

The hyperfine coupling constants $A_\perp$, $A_\parallel$, C, and D, which enter the SMR Hamiltonian, Eq. (2), were determined using the Knight shift measurements in $YBa_2Cu_3O_7$ and the frequency of the antiferromagnetic resonance in $YBa_2Cu_3O_6$.[10,29] The momentum dependence of the form factors is shown in Fig. 5. A striking difference of the temperature dependence and the magnitude of the spin-lattice relaxation on the ^{63}Cu, ^{17}O, and ^{89}Y nuclei led Millis *et al.*[10] to the conclusion that the magnetic response function is strongly peaked at the antiferromagnetic wave vector, as might be expected if one were close to an antiferromagnetic singularity. Since the form factors for ^{17}O and ^{89}Y nuclei vanish at $\mathbf{Q}=(\pi/a,\pi/a)$, the difference in the magnitude and temperature dependence of ^{63}Cu and other relaxation rates can be easily explained. Once the assumption of strong enhancement of the magnetic response function at the antiferromagnetic wave vector is made, the ^{63}Cu spin-lattice relaxation anisotropy ratio provides a self-consistency check on the values of the hyperfine constants,

$$ {}^{63}R=\frac{T_{1\parallel}}{T_{1\perp}}=\frac{{}^{63}F_\perp(\mathbf{Q})}{{}^{63}F_\parallel(\mathbf{Q})}\simeq 3.7. \tag{7}$$

The values of the hyperfine constants,

$$ B=3.82\times 10^{-7}\ \text{eV}, \quad A_\parallel=-4B, $$

$$ A_\perp=0.84B, \quad C_\parallel=0.91B, \tag{8}$$

satisfy this check. Moreover, these hyperfine coupling constants remain unchanged (at the 5% to 10% level) with the variation of the doping level or for different cuprate materials, as might be expected from quantum chemical arguments. Thus these constants can be regarded as the same for both the $YBa_2Cu_3O_{6+x}$ and $La_{2-x}Sr_xCuO_4$ families.

We follow Millis *et al.*[10] and Monien *et al.*[29] and use a response function consisting of an anomalous part $\chi_{\rm MMP}(\mathbf{q},\omega)$ and a Fermi-liquid part $\chi_{\rm FL}(\mathbf{q},\omega)$,

$$\chi(\mathbf{q},\omega)=\chi_{\mathrm{MMP}}(\mathbf{q},\omega)+\chi_{\mathrm{FL}}(\mathbf{q},\omega). \tag{9}$$

The expression used by Millis *et al.*[10] for the anomalous part can be written in the mean-field form:

$$\chi(\mathbf{q},\omega)_{\mathrm{MMP}}=\frac{\chi_Q}{1+(\mathbf{q}-\mathbf{Q})^2\xi^2-i\omega/\omega_{\mathrm{SF}}}, \tag{10}$$

where

$$\chi_Q=\alpha\xi^2. \tag{11}$$

Here ω_{SF} is the characteristic frequency of the spin fluctuations, ξ is the correlation length, and α is a scale factor. Due to the strong antiferromagnetic enhancement, the anomalous contribution to the copper relaxation rate dominates at all doping levels. However, since the form factors for other nuclei are zero at the antiferromagnetic wave vector, the Fermi liquid (Korringa-like) contribution to their spin-lattice relaxation rate becomes important.

In the limit of long correlation lengths the expressions for the ^{63}Cu relaxation rates, Eqs. (4), (6), are considerably simplified:[28]

$$^{63}(T_1T)=132(\mathrm{s\ K})/\mathrm{eV}^2\omega_{\mathrm{SF}}/\alpha, \tag{12}$$

while

$$^{63}\frac{1}{T_{2G}}=295(\mathrm{eV/s})\alpha\xi\ . \tag{13}$$

Thus, up to a scale factor α, $^{63}(T_1T)$ provides a direct measurement of ω_{SF}, while $^{63}T_{2G}$ provides a measurement of the correlation length. Moreover, the ratios

$$\frac{^{63}T_1T}{^{63}T_{2G}}=3.9\times10^4(\mathrm{K/eV})(\omega_{\mathrm{SF}}\xi=c'), \tag{14}$$

$$\frac{^{63}T_1T}{^{63}T_{2G}^2}=1.15\times10^7(\mathrm{K/s})(\alpha\omega_{\mathrm{SF}}\xi^2=\chi_Q\omega_{\mathrm{SF}}) \tag{15}$$

tell us about the scaling laws,[9] if any, obeyed by the low-frequency magnetic excitations. Thus, as emphasized in Refs. 9,30 if $^{63}T_1T/T_{2G}$ is independent of temperature, one has QC $z=1$ scaling behavior, and the doping-dependent ratio $\omega_{\mathrm{SF}}\xi=c'$ is determined. On the other hand, when $^{63}T_1T/^{63}T_{2G}^2=$const, ω_{SF} displays either nonuniversal mean field or QC $z=2$ scaling behavior, and the product $\chi_Q\omega_{\mathrm{SF}}$ is independent of temperature.

III. EXPERIMENTAL PHASE DIAGRAMS

In this section we use the NMR results for $^{63}T_1$, $^{63}T_{2G}$, and the Knight shift on the underdoped 1-2-3 and the 2-1-4 families to establish the complete experimental magnetic phase diagram for these systems. We first review briefly the properties of the regimes which might be relevant to the experimental situation in the metallic cuprates.[9]

(i) The QC, $z=1$ regime. In this regime the spin-spin correlator takes the form

$$\chi(\mathbf{q},\omega)=\xi^{2-\eta}F(\mathbf{q}\xi,\omega\xi), \tag{16}$$

and the inverse correlation length varies linearly with temperature, $1/\xi=aT+b$, where in the σ model[6] a and b are computable universal constants. The key signature of the QC $z=1$ regime in NMR measurements[9] is that the ratio $^{63}T_1T/^{63}T_{2G}\propto\omega_{\mathrm{SF}}\xi=c'$ is temperature-independent [Eq. (15)], and c' is, for the σ model, proportional to the spin-wave velocity c, $c'\simeq0.55c$. In the QC regime the characteristic frequency ω_{SF} is linear in temperature. The bulk magnetic susceptibility should also vary linearly with temperature,

$$\chi(T)=\chi_{\mathrm{univ}}(T)+\chi_0, \tag{17}$$

where $\chi_{\mathrm{univ}}(T)$ is a universal linear contribution, computable in the σ model:[6]

$$\chi_{\mathrm{univ}}(T)=\left(\frac{g\mu_B}{\hbar c}\right)^2[0.34k_BT-0.137\Delta(T=0)], \tag{18}$$

while χ_0, the fermionic contribution, is temperature independent.

(ii) The quantum critical, $z=2$, regime.[10,15] The characteristic energy scale in this regime is again set by temperature, so that at high enough temperatures $\omega_{\mathrm{SF}}\propto T$. However, since $z=2$, $\omega_{\mathrm{SF}}\propto\xi^{-2}$. As a result, in this regime $^{63}T_1T/^{63}T_{2G}^2=$const, and at high temperatures the inverse squared correlation length should obey the Curie-Weiss law $\xi^{-2}=aT+b$.

(iii) The QD regime. In this regime the correlation length (and $^{63}T_{2G}$) saturates. If $z=2$, the damping frequency ω_{SF} (and $^{63}T_1T$) should saturate at zero temperature to a certain value, determined by the fermionic damping.[13,14] In case of the $z=1$ σ model, ω_{SF} in the QD regime increases exponentially with decreasing temperature.[6]

(iv) Nonscaling regime. In this regime lattice effects are appreciable, and a scaling analysis is inapplicable. As a result, the calculations in this regime are model dependent. A subclass of the nonscaling regime is the mean-field NAFL at high doping, where Eq. (10) can be used.

In order to describe the $z=2$ regime, the σ model, Eq. (1), should be generalized to include fermionic damping.[14] The effect of this damping is that at low enough temperatures one always should find a crossover from the $z=1$ to $z=2$ scaling regime. This crossover happens either in the QC or the QD regime, depending on the value of the fermionic damping. We briefly discuss this model in Sec. IV.

We begin our analysis of magnetic behavior by considering $La_{2-x}Sr_xCuO_4$, where the spin susceptibility χ_0 has been measured both in the bulk experiments[18,24] and in NMR Knight shift probes,[19,26] and $^{63}T_1$ measurements have been carried out for many different doping levels.[7,31] The decrease in the spin susceptibility as the temperature is lowered over a broad temperature region was the first identification in the experimental literature of the "spin pseudogap" phenomenon. At a temperature T_χ, the spin susceptibility (or the ^{63}Cu Knight shift) which at high temperatures typically decreases somewhat with increasing temperature, as shown in Figs. 6 and 7, changes behavior; below T_χ it decreases as temperature is lowered. Loram *et al.*[20] have carried out specific heat measurements which show that this decrease in χ_0 is matched by a corresponding decrease in the quasiparticle density of states, $N_0(T)$. Johnston[18] and subsequently Nakano *et al.*[24] also found that the bulk magnetic susceptibility could be expressed in a scaling form:

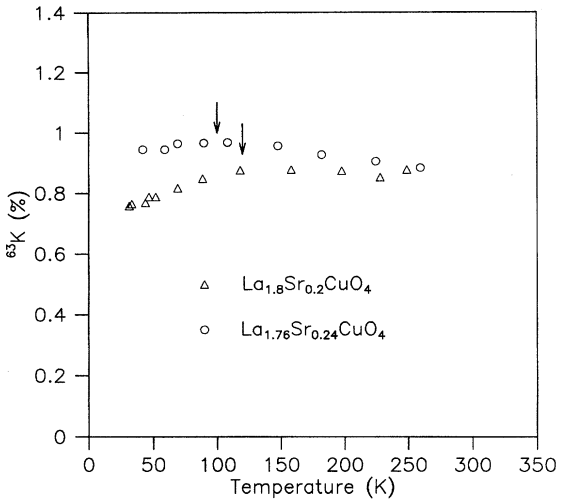

FIG. 6. T_{cr} (denoted by arrows) for $La_{1.8}Sr_{0.2}CuO_4$ and $La_{1.76}Sr_{0.24}CuO_4$, as determined from the endpoint of linear in T behavior and the maximum of the ^{63}Cu Knight shift measured by Ohsugi *et al.* (Ref. 31).

$$\chi(T)=\chi_0+\kappa\chi(T/T_{\max}). \tag{19}$$

Nakano *et al.*[24] used χ_0, κ, and $T_{\max}$ as fitting parameters. They found that the temperature-independent term χ_0 is doping dependent; it therefore cannot be ascribed to the Van Vleck contribution. This scaling behavior is easily explained if one identifies χ_0 as the "fermionic" part, and $\kappa\chi(T/T_{\max})$ as the "spin" part. Equation (19) is then quite similar to Eq. (17), the result expected from the scaling theory. However, it should be emphasized that from our point of view, because of large lattice corrections, scaling ends above some temperature T_{cr}. To preserve Eq. (19), the lattice corrections should enter "universally," i.e., preserving the relationship (17), while breaking the σ-model linear temperature dependence of $\chi_{\text{univ}}(T)$.

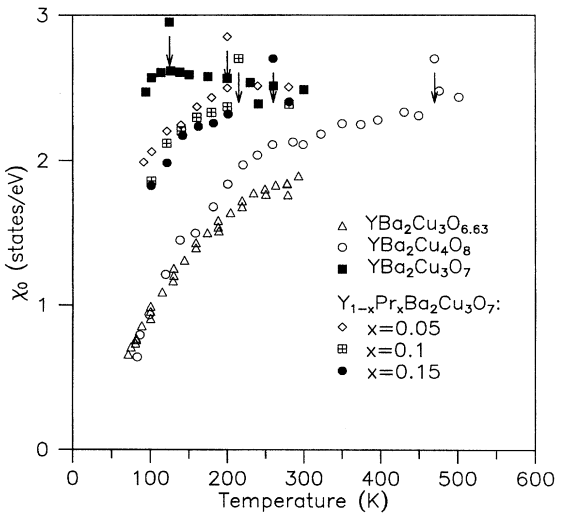

FIG. 7. The spin susceptibility inferred from the Knight shift data for $YBa_2Cu_3O_{6.63}$, $YBa_2Cu_4O_8$, $YBa_2Cu_3O_7$, and $Y_{1-x}Pr_xBa_2Cu_3O_7$, with $x=0.05,0.1,0.15$.

Quite generally, for a $z=1$ scaling regime which extends between a lower crossover temperature T_* and an upper crossover temperature T_{cr}, one expects scaling behavior to manifest itself at both long wavelengths [i.e., in $\chi_0(T)$] and at the wave vectors around **Q** which determine both $^{63}T_1$ and $^{63}T_{2G}$, with both $\chi_0(T)$ and $^{63}T_1T$ exhibiting a linear temperature dependence. T_{cr} marks the onset of scaling behavior, while T_* marks beginning of the crossover from the QC ($z=1$) to the QD regime, predicted in the scaling theory,[3] which has been previously identified in the NMR $^{63}T_1$ and $^{63}T_{2G}$ data.[9,13] This is the temperature at which $^{63}T_1T$ and $^{63}T_{2G}$ stop being linear in T, as is expected for the QC $z=1$ regime. We propose that T_{cr} marks the crossover from scaling and spin pseudogap behavior to nonuniversal behavior. Inspection of Fig. 6 then show that T_{cr} cannot be far from T_χ; in other words, the maximum in $\chi_0(T)$ is reached at very nearly the same temperature at which scaling begins. Inspection of Fig. 8 shows that the crossover at T_{cr} is also visible in $^{63}T_1T$, as a change in slope; for the various samples for which both $\chi_0(T)$ and $^{63}T_1$ measurements have been carried out, the two independent methods (one long wavelength, one short wavelength) of determining T_{cr} are seen to be in good agreement with one another. The lower crossover, at T_*, is readily visible in the $^{63}T_1$ data of Ohsugi *et al.*[31] and Imai *et al.*[7] shown in Fig. 8. It is also clearly visible in $\chi_0(T)$ measurements for Sr doping levels, 0.15 and below, as marking the onset of a more rapid falloff in $\chi_0(T)$ as the temperature is further decreased. Our experimentally determined values of T_* and T_{cr} are given in Fig. 3; T_* is seen to vary comparatively slowly with hole concentration; it possesses a maximum for doping levels in the vicinity of $La_{1.85}Sr_{0.15}CuO_4$. T_{cr} on the other hand varies rapidly with hole concentration, for doping levels less than $La_{1.8}Sr_{0.2}CuO_4$. We indicate by a solid line our linear extrapolation of T_{cr} to doping levels less than $La_{1.85}Sr_{0.15}CuO_4$ (where high temperature measurements of $^{63}T_1$ have not yet been carried out); we note that this extrapolation suggests a crossover temperature of ~ 1200 K for the AF insulator La_2CuO_4 not far from that found from the high-temperature series studies of the 2D Heisenberg antiferromagnet.[32]

Spin pseudogap and scaling behavior has also been found in transport measurements on the 2-1-4 system. Hwang *et al.*[23] and Nakano *et al.*[24] analyzed the data for the bulk magnetic susceptibility, resistivity,[24] and Hall effect[24,23] measurements for this system. They identified T_χ from the spin susceptibility, and found similar characteristic temperatures T_ρ and T_H from an analysis of change with temperature of the resistivity and Hall effect. It is not necessary, from our point of view, that the temperatures identified using these criteria be exactly the same. However, as may be seen in Fig. 4, where our suggested doping dependence of T_{cr} is compared with T_χ, T_ρ, and T_{R_H}, these respective temperatures are very close to each other, a closeness which makes evident the inseparability of spin and charge behavior in this system. We note that due to the vague nature of the crossovers large errors of $\sim 15\%$ are involved in our estimates for the values of crossover temperatures. Errors may also occur because the doping is not always exactly known, while different measurements are often performed on different samples.

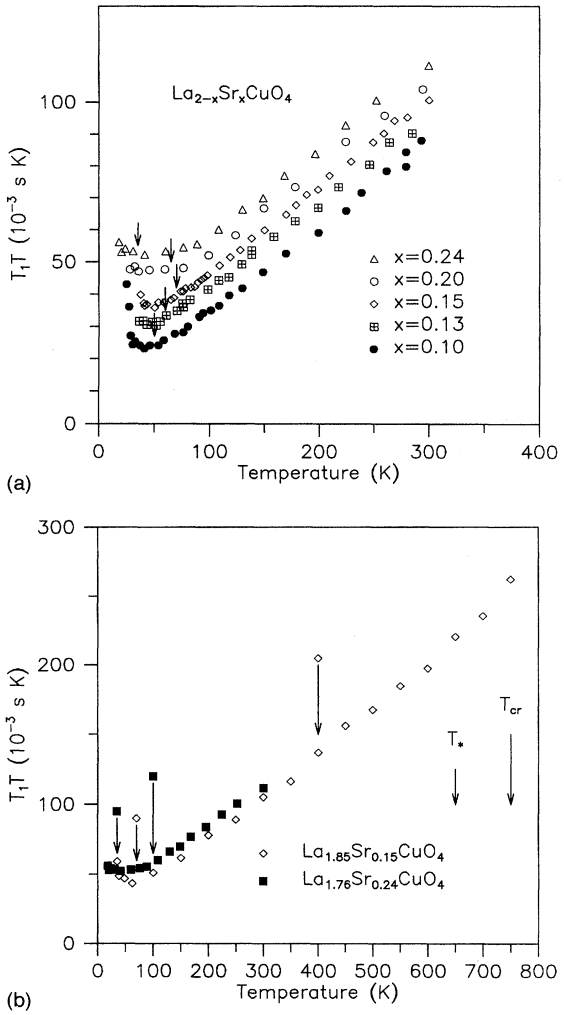

FIG. 8. The temperature T_* (denoted by arrows) for the QC-QD crossover, as determined from the $^{63}T_1T$ measurements of Ohsugi *et al.* (Ref. 31) (a) and Imai *et al.* (Ref. 7) (b) in $La_{2-x}Sr_xCuO_4$.

Having established that the phenomena of scaling and spin pseudogap behavior are intimately related, and that both begin at T_{cr}, we next explore the possibility suggested by Monthoux and Pines,[17] that T_{cr} is associated with a critical value of the correlation length ξ_{cr} which is independent of doping. One reaches the same conclusion on the basis of the σ model, where one argues that lattice corrections bring about an end to scaling for $\xi > \sim 1$. We make the ansatz that $\xi_{cr} \simeq 2$. Our reason for choosing this value is that one finds that in both the insulating and nearly fully doped samples, the onset of spin pseudogap behavior coincides with $\xi \simeq 2$. Thus, in the insulator, the bulk susceptibility reaches its maximum at $T \sim 1400$ K,[18] not far from the temperature ($T_{cr} \simeq 1000$ K) at which $\xi = 2$ according to high-temperature series studies,[32] while, as we shall see below, at the opposite end of the doping scale, $\xi \simeq 2$ at the temperature (125 K) which marks the onset of spin pseudogap behavior in almost fully doped $YBa_2Cu_3O_7$.

Unfortunately, $^{63}T_{2G}$ data is not yet available in the metallic 2:1:4 samples, so that one cannot verify directly (as we shall be able to do for their 1:2:3 counterparts) that the scaling law $\omega_{SF}\xi = c'$, a constant, is obeyed for these systems. However, on the assumption that it is valid, and moreover that $\xi_{cr} = 2$, we can determine the correlation length in the QC regime based on the NMR $^{63}T_1$ measurements only. To see this, note that between T_* and T_{cr} we have

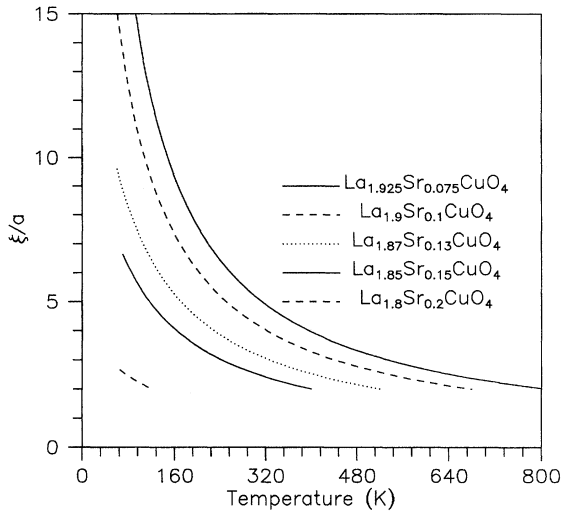

FIG. 9. The temperature dependence of the correlation length in the QC regime, obtained by us for the $La_{2-x}Sr_xCuO_4$ system.

$$^{63}T_1(T)T = 132(\text{s K})\frac{c'}{\alpha\xi(T)} \quad (T_* \leq T \leq T_{cr}), \tag{20}$$

so that a knowledge of T_{cr} from another experiment [e. g., the maximum in $\chi_0(T)$] serves to fix c'/α, and hence $\xi(T)$. The doping dependence of c'/α can also be determined from $^{63}T_1T$ only, since

$$\frac{c'}{\alpha} = {}^{63}[T_1(T_{cr})T_{cr}]\frac{eV^2}{66 \text{ s K}}. \tag{21}$$

The correlation length as a function of temperature and c'/α for different doping levels are shown in Figs. 9,10.

It is instructive to consider the extent to which the values of $\xi(T)$ we have determined from $^{63}T_1$ display the universal behavior predicted by the σ model for the $z=1$ scaling regime $\xi^{-1} = a + bT$ for the case in which c and c' do not vary with doping. We see from Table I that the coefficients a and b are not universal, which is a clear indication that c, c', and hence α, must be doping dependent in this system. On the other hand, we find that the slope of $^{63}T_1T$ is nearly doping independent between T_* and T_{cr} [$^{63}T_1T$(ms K) $= 28 + 0.027T$ for $La_{1.9}Sr_{0.1}CuO_4$ and $^{63}T_1T$(ms K) $= 10 + 0.025T$ for $La_{1.76}Sr_{0.24}CuO_4$], which is what scaling theory for a doping-dependent c would predict. We note that our assumption that $\xi \simeq 2$ at T_{cr} means that ξ^{-1} may be written in a simple form

$$\frac{1}{\xi} = a + (\tfrac{1}{2} - a)(T/T_{cr}), \tag{22}$$

which experiments given in Table I satisfy.

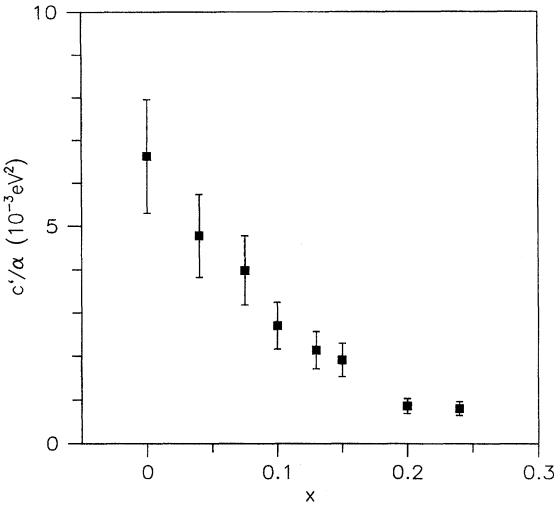

FIG. 10. The variation of c'/α with doping in $La_{2-x}Sr_xCuO_4$.

We turn next to the $YBa_2Cu_3O_{6+x}$ family. A complete analysis can be done for the compounds $YBa_2Cu_3O_{6.63}$, $YBa_2Cu_4O_8$, and $YBa_2Cu_3O_7$, where $^{63}T_1$, $^{63}T_{2G}$, and Knight shift data are available. A less complete analysis, comparable to that given above for the 2-1-4 system, can be given for the Pr-doped $YBa_2Cu_3O_7$, where only $^{63}T_1$ and Knight shift experiments have been carried out. We start by analyzing the Knight shift experiments in the Pr-doped compounds $Y_{1-x}Pr_xBa_2Cu_3O_7$,[33] with $x=0.05$, 0.1, and 0.15. We assume that Pr substitution acts to remove, on average, 1/2 hole per plane for each substituted Pr atom. Thus the planar hole concentration in $Y_{1.95}Pr_{0.05}Cu_3O_7$ is assumed to be 0.025 less than that of the "host" material $YBa_2Cu_3O_7$. But, as noted above, the hole concentration of that material is not precisely known, so that a corresponding degree of uncertainty affects the doping dependence we propose for this system. The spin part of the bulk magnetic susceptibility we obtain for these compounds (in states/eV) is shown in Fig. 7. As we have done for the 2-1-4 system, we identify the onset of scaling behavior T_{cr}, with the maximum T_χ of the curve $\chi_0(T)$. We note that the bulk spin susceptibility varies linearly with temperature between T_* and T_{cr}, as expected for the scaling regime. On turning to the $^{63}T_1T$ plots, shown in Figs. 11(a), 12, we see that the lower crossover temperature T_* is clearly visible, while, just as was the case for the 2-1-4 system, the crossover temperature, T_{cr}, at which $^{63}T_1T$ changes slope, is barely discernable. As we did for the 2-1-4 system, once T_{cr} is identified, we can determine the doping dependence of both c'/α and $1/\xi$ for these systems, with the results given in Table I.

We next consider $YBa_2Cu_3O_7$, for which measurements of the Knight shift,[34] $^{63}T_1$, and $^{63}T_{2G}$ have been carried out. The experimental results of Imai and Slichter[35] for $^{63}T_{2G}$ and $^{63}T_1T$ in $YBa_2Cu_3O_7$ bring out two important points.

(i) For $T \geq 125$ K, ω_{SF} and ξ^{-2} display Curie-Weiss (linear in T) behavior (Figs. 13, 14).

(ii) For $T \geq 125$ K $\omega_{SF}\xi^2 = \text{const}$. This behavior, which has been previously identified as the Gaussian, $z=2$, scaling regime, could equally well be regarded as a manifestation of nonuniversal mean field behavior.[10]

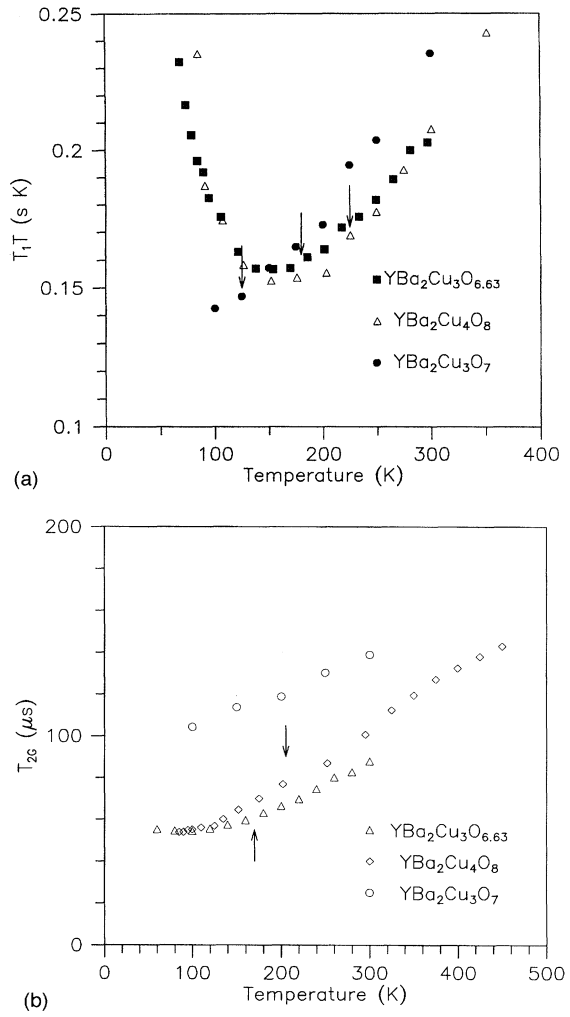

FIG. 11. The determination of T_*, the QC-QD crossover, for the three compounds $YBa_2Cu_3O_{6.63}$, $YBa_2Cu_4O_8$, and $YBa_2Cu_3O_7$: (a) from $^{63}T_1$ measurements, (b) from $^{63}T_{2G}$ measurements.

What happens at 125 K, where $^{63}T_1T$ stops being linear in T? The results of Walstedt *et al.*[34] provide an essential clue. For their sample, as shown in Fig. 13, the bulk spin susceptibility displays only a minor variation with temperature in $YBa_2Cu_3O_7$, with a comparatively shallow maximum at 125 K. However, at lower temperatures the variation of the spin susceptibility becomes much more pronounced. We therefore identify T_{cr} as ~ 125 K for the doping level present in this sample, which may be slightly on the underdoped side. Our ansatz that $\xi=2$ at 125 K then permits us to determine α directly from the $^{63}T_{2G}$ measurements of Imai *et al.*;[35] we obtain $\alpha=15.6$ states/eV, a value slightly larger than that previously adapted by Thelen and Pines,[28] while, on making use of (Eq). 21, we find $c'=35$ meV for this material.

Our conclusion that $T_{cr}=125$ K for "$YBa_2Cu_3O_7$" thus assigns it a place as a full member of the 1:2:3 family, exhibiting the same magnetic scaling and spin pseudogap behavior as the underdoped system $Y_{0.95}Pr_{0.05}Ba_2Cu_3O_7$, but

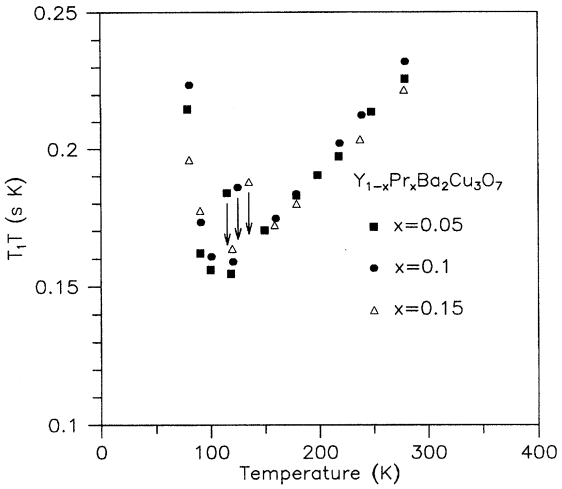

FIG. 12. The determination of T_*, the QC-QD crossover, from $^{63}T_1$ measurements on $Y_{1-x}Pr_xBa_2Cu_3O_7$.

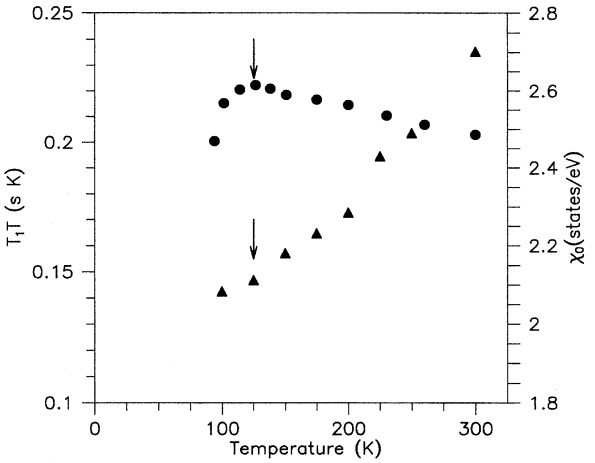

FIG. 13. The crossover behavior at 125 K displayed by the spin contribution to the magnetic susceptibility (Ref. 37) and $^{63}T_1T$ (Ref. 35) in $YBa_2Cu_3O_7$.

with a substantially lower value of T_{cr}. Viewed from this perspective, the $^{63}T_{2G}$ measurements of Imai *et al.*[35] confirm our tentative hypothesis that the crossover at T_{cr} is to a non-universal mean-field regime. In order to examine more closely the doping dependence of T_{cr} for this family, we need to know the oxygen doping level of the samples studied by Walstedt *et al.*[34] and Imai *et al.*[35] In the absence of detailed experimental information, we assume these correspond to $YBa_2Cu_3O_{6.95}$, although a somewhat lower oxygen doping level would be equally plausible. We then obtain the results for the doping dependence of T_{cr} and (c'/α) for the 1:2:3 family shown in Figs. 2 and 15.

We next consider $YBa_2Cu_4O_8$, a material which possesses the same planar hole concentration as $YBa_2Cu_3O_{6.8}$, for which both NQR and NMR measurements of $^{63}T_1$ and $^{63}T_{2G}$ have been carried out by Corey *et al.*,[36] with the results given in Fig. 11(a),(b). They obtain the very important result that within experimental error the ratio $(^{63}T_1T/T_{2G})$ is constant between 215 and 450 K, thus demonstrating that $YBa_2Cu_4O_8$ exhibits scaling behavior over a broad temperature range, between $T_*=215$ K and $T_{cr}\geq 450$ K. Our examination of the Knight shift results of Zimmerman[37] suggests to us that $\chi(T)$ reaches its maximum value near 500 K, so that $T_\chi \simeq 500$ K; we therefore adopt the value, $T_{cr}=470$ K and use this assignment to obtain $c'/\alpha=4.57$, from an extrapolation of the results for $^{63}T_1$ to this temperature. From the $^{63}T_{2G}$ results of Corey *et al.*,[36] we find $c'=50$ meV and $\alpha=10.9$ states/eV for this material, while the temperature variation of ξ is given in Table I and Fig. 16.

The final member of the 1:2:3 family for which $^{63}T_{2G}$ measurements have been carried out is $YBa_2Cu_3O_{6.63}$, where the measurements of Takigawa[8] were used by Sokol and Pines[9] to establish scaling behavior, with $T_*\simeq 170$ K. Because high-temperature ($T>500$ K) measurements of $^{63}T_1$ $^{63}T_{2G}$, or χ are not available for this system, one cannot obtain T_{cr} from experiment. However, on assuming that T_{cr} continues to vary linearly with oxygen doping, as Fig. 2 suggests that it does between $YBa_2Cu_4O_8$ and $YBa_2Cu_3O_{6.95}$, we find $T_{cr}=(840\pm 150)$ K, with the corresponding results for c', α, and $1/\xi$ given in Table I and Figs. 16, 17. Our results for the doping dependence of c' and α show that while c' decreases with increased oxygen content, α increases in such a way that the product $\alpha c'$ is nearly constant, a result we examine further in the following section.

Our determination of the dependence of T_{cr} on oxygen

TABLE I. Spin fluctuation parameters determined from fits to NMR experiments.

System	T_{cr} (K)	T_* (K)	c'/α (10^{-3} eV^2)	α (states/eV)	c' (meV)	$\alpha c'$	$1/\xi$ ($T_*\lesssim T\lesssim T_{cr}$)
$YBa_2Cu_3O_{6.63}$	840	170	7.67	8.34	64	0.53	$0.052+5.93\times10^{-4}T$
$YBa_2Cu_4O_8$	470	215	4.57	10.9	50	0.545	$0.068+9.2\times10^{-4}T$
$YBa_2Cu_3O_7$	125	–	2.23	15.6	35	0.545	–
$Y_{0.95}Pr_{0.05}Ba_2Cu_3O_7$	200	115	2.83	–	–	–	$0.32+9.0\times10^{-4}T$
$Y_{0.9}Pr_{0.1}Ba_2Cu_3O_7$	215	125	3.0	–	–	–	$0.31+8.8\times10^{-4}T$
$Y_{0.85}Pr_{0.15}Ba_2Cu_3O_7$	260	130	3.18	–	–	–	$0.29+8.1\times10^{-4}T$
$La_{1.9}Sr_{0.1}CuO_4$	680	50	2.7	–	–	–	$0.024+7.01\times10^{-4}T$
$La_{1.85}Sr_{0.15}CuO_4$	410	70	1.91	–	–	–	$0.065+1.06\times10^{-3}T$
$La_{1.8}Sr_{0.2}CuO_4$	120	65	0.86	–	–	–	$0.23+2.25\times10^{-3}T$
$La_{1.76}Sr_{0.24}CuO_4$	100	35	0.83	–	–	–	$0.255+2.46\times10^{-3}T$

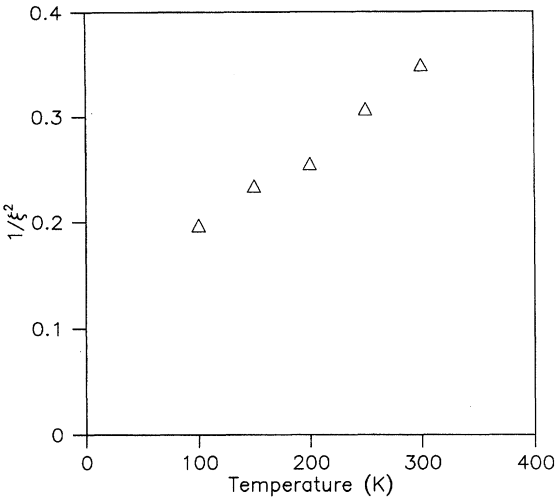

FIG. 14. The Curie-Weiss temperature dependence for ξ^2 determined from the $^{63}T_{2G}$ measurements of Imai *et al.* (Ref. 35) in $YBa_2Cu_3O_7$.

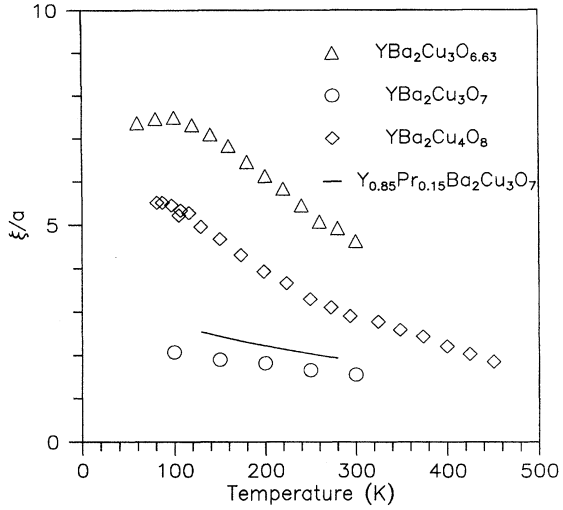

FIG. 16. The antiferromagnetic correlation length in the $YBa_2Cu_3O_{7-\delta}$ system, as determined from the $^{63}T_{2G}$ measurements. For the Pr-doped compound (the line) the correlation length in the QC regime was determined from the $^{63}T_1T$ measurements.

doping for the 1:2:3 system makes clear the hierarchy of antiferromagnetic correlations shown in Fig. 16, in which, at a given temperature, ξ increases rapidly as the planar hole concentration is reduced. It also enables us to compare 1:2:3 system with the 2:1:4 system. To do so, we choose $YBa_2Cu_3O_{6.5}$ as a basis, arguing that up to this oxygen concentration oxygen atoms added to the insulator $YBa_2Cu_3O_6$ go primarily into chain or interstitial positions, leaving the hole concentration in the plane near zero. We then assume one hole per plane for each added oxygen, so that $YBa_2Cu_3O_{6.95}$ corresponds to a hole concentration $n_h=0.225$, etc., while for the $La_{2-x}Sr_xCuO_4$ system we assume that each added Sr atom introduces a hole in the plane. The resulting dependence of T_{cr} on hole concentration is given in Fig. 4. We see that within the not inconsiderable uncertainties of T_{cr} and hole concentration, the two families

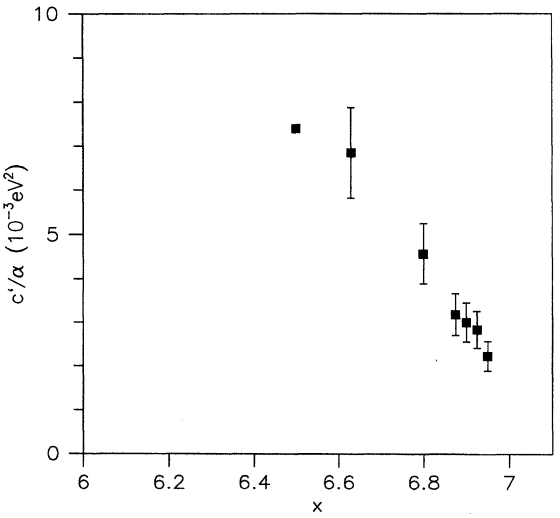

FIG. 15. c'/α, determined from the $^{63}T_1$ measurements, as a function of doping in $YBa_2Cu_3O_{7-\delta}$.

display the same dependence of T_{cr} on hole concentration. These results lead us to two important conclusions

(i) Despite their somewhat different band structure and Fermi surfaces, the 2:1:4 system and 1:2:3 system possess essentially the same magnetic phase diagram. Put another way, that diagram is only very weakly dependent on band structure; it simply reflects the planar hole concentration.

(ii) The bilayer couplings[30] found in neutron scattering experiments on the 1:2:3 system plays little or no role in determining spin pseudogap and scaling behavior.

IV. THEORETICAL MODEL

Several models have been applied to describe the spin fluctuations in the metallic state. Two that appear consistent with experimental picture described above are the σ model[3,6] and the nearly antiferromagnetic Fermi-liquid (NAFL) description. The starting point of the σ model is a set of localized spins interacting with the fermionic background. It is possible then to integrate out fermions, so that one is left with the action of the ordering field. It can be shown that the σ model action, Eq. (1), should then be generalized to include the effect of quasiparticle damping, if this kind of damping is allowed by conservation laws. This leads to a description of the $z=1$ to $z=2$ crossover.[14] If the quasiparticle source of damping is absent, the fermions just change the σ-model coupling constant and the spin-wave velocity. This model relies heavily on the existence of the propagating spin-wave excitations in the metallic state, which so far has not been unambiguously confirmed in the direct experiments. In the NAFL description such spin-wave excitations are not needed, but can arise as a result of a frequency-dependent effective interaction. The "spin pseudogap" is then related to a nonlinear feedback effect which brings about the equivalent of $z=1$ scaling. We believe that both models describe from different viewpoints the same physics of the propagating spin excitations in the metallic underdoped cuprates. We

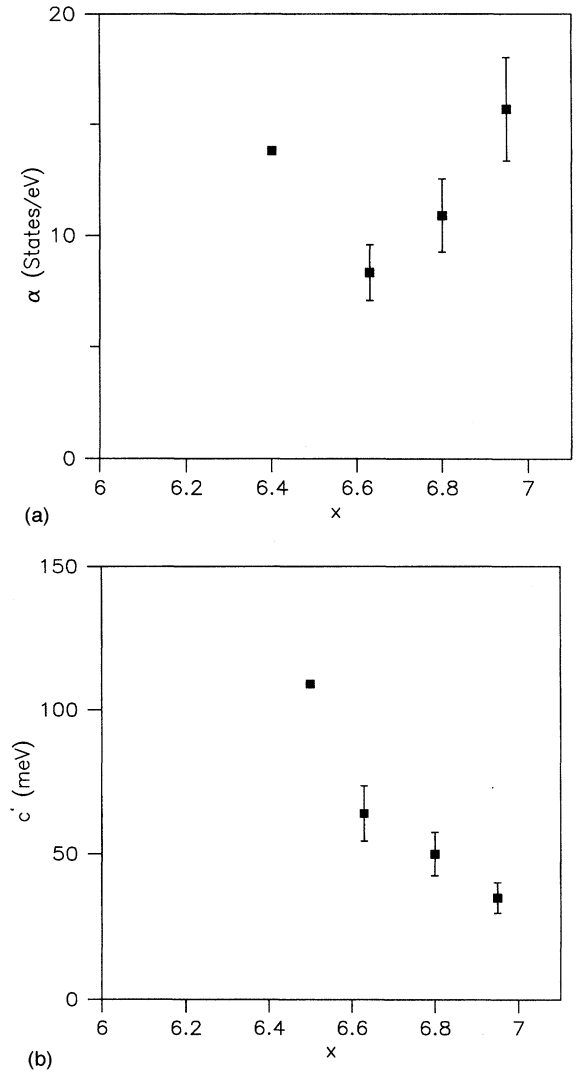

FIG. 17. The parameters α (a) and c' (b), determined for the three compounds $YBa_2Cu_3O_{6.63}$, $YBa_2Cu_4O_8$, and $YBa_2Cu_4O_7$, where both $^{63}T_1$ and $^{63}T_{2G}$ relaxation time measurements are available.

now consider those in more detail, with particular attention to the generalization of the MMP model, Eq. (10), to finite frequencies, in order to be able to compare the model prediction with the results of neutron-scattering experiments.

A. QNLσM plus holes

In this subsection we discuss the spin-fermion model. We assume that the fermionic and spin degrees of freedom can be separated, and the action for the spins is the σ model. We further assume a specific form for the interaction between the fermion and spin degrees of freedom:

$$H_{\rm int}=J_0\sum_{ij}\psi_i^+(\boldsymbol{\sigma}_{ij}\mathbf{S})\psi_j, \tag{23}$$

where the ij are the spin indices.

It can be shown[38] that integrating out fermions leads to the following action in this model:[14]

$$S=\frac{1}{2g}T\sum_{\omega_n}\int\frac{d^2q}{4\pi^2}|\mathbf{n}(\mathbf{q},\omega_n)|^2\left(c_0q^2+\frac{\omega_n^2}{c_0}+\gamma|\omega_n|\right). \tag{24}$$

Here both g and c_0 are renormalized by fermions. Quasiparticles also lead to an additional damping, the $\gamma|\omega_n|$ term in the action, if this kind of damping is allowed by the conservation laws. The σ-model constraint $|n|=1$ remains valid in this case.

Applicable to systems with two components,[39] the decomposition of the one-component system in two components, the "spins" $\mathbf{S}$ and the "fermions" ψ could be artificial. In fact, at high doping $YBa_2Cu_3O_{6+x}$ is known to be a one-component system, where the Fermi surface is measured in the ARPES experiments.[40] There is no proof that the model Eq. (24) applies in the one-component case, although some arguments in its favor have been given by Sachdev *et al.*[14] The necessary condition for the model Eq. (24) to be valid is, in our opinion, an almost local character of the copper spins.

The scaling analysis of the model[14] specified by Eq. (24) leads to a magnetic susceptibility near the ordering wave vector (π,π) which is a universal function:

$$\chi(\mathbf{q},\omega)=\frac{Z}{(k_BT)^{-\eta}}\left(\frac{\hbar c}{k_BT}\right)^2\Phi_s\left(\frac{q}{T},\frac{\omega}{T},\frac{\Delta_0}{T},\frac{\Gamma}{T}\right). \tag{25}$$

Here q marks the deviation from the ordering wave vector (π,π). The two energy scales $\Delta(T=0)$ and Γ reflect the energy gap in the spin-wave spectrum and the strength of the fermionic damping, respectively. The scaling analysis[14] shows that fermions do not necessarily overdamp and destroy the spin waves. At low damping the crossover is the same as in the pure σ model. The only difference is in the presence of a finite fermionic damping in the QD regime. At higher Γ, there are two crossovers with decreasing temperature. The first one, from the high-temperature QC $z=1$ to the low-temperature QC $z=2$ regime, happens at $T\sim\Gamma$. At this temperature, according to this analysis, the temperature dependence of the correlation length $\xi\propto 1/T$ should change to $\xi^2\propto 1/T$. The lower second crossover at $T\sim\Delta^2/\Gamma$ corresponds to the onset of the QD $z=2$ regime.

As is the case for the pure σ model,[6] the σ model with fermionic damping, Eq. (24), can be approached using a $1/N$ expansion technique. For $N=\infty$, the resulting magnetic susceptibility takes the form[13]

$$\chi(\mathbf{q},\omega)=\frac{\alpha\xi^2}{1+(\mathbf{q}-\mathbf{Q})^2\xi^2-\dfrac{\omega^2}{\Delta^2}-i\dfrac{\omega}{\omega_{\rm SF}}}. \tag{26}$$

Here $\omega_{\rm SF}\propto\xi^{-2}$ is the characteristic frequency of the damping in the particle-hole channel; $\Delta=c/\xi$ is the value of the actual gap in the spectrum of the spin-wave excitations of the disordered state. Equation (26) can be understood as a mean-field propagator for the spin excitations damped in quasiparticle channel.[13,41] Note that the only source of damping in mean-field theory is the decay of spin wave into two fermions. Another source of damping, multiple spin-wave scattering, appears only beyond the mean field, in the first order in $1/N$. On the contrary, the energy spectrum of the disordered

magnons is already adequate in the mean-field approximation.[32] To summarize these considerations, we therefore write

$$\frac{1}{\omega_{\rm SF}(\mathbf{q},\omega)}=\frac{1}{\omega_{\rm fermion}}+\frac{1}{\omega_{\rm spin}(\mathbf{q}\xi,\omega/\Delta)}\,, \tag{27}$$

where $\omega_{\rm fermion}$ is the fermionic damping frequency appearing in the mean field theory, while $\omega_{\rm spin}$ appears as a result of $1/N$ corrections, and displays spatial and frequency dependence on the scale of the correlation length.

The imaginary part of Eq. (26) has the form

$$\chi''(\mathbf{q},\omega)=\frac{\alpha\xi^2\dfrac{\omega}{\omega_{\rm SF}}}{\left(1+q^2\xi^2-\dfrac{\omega^2}{\Delta^2}\right)^2+\dfrac{\omega^2}{\omega_{\rm SF}^2}}, \tag{28}$$

from which we obtain the integrated (or local) magnetic susceptibility

$$\chi_L''(\omega)=\pi\alpha\left(\frac{\pi}{2}-\tan^{-1}\left[\frac{\omega_{\rm SF}}{\omega}-\frac{\omega\omega_{\rm SF}}{\Delta^2}\right]\right). \tag{29}$$

Note that for $\omega>\Delta$ the imaginary part of the magnetic susceptibility Eq. (28) is peaked at an incommensurate wave vector, which is just a reflection of the spin waves at high energy. This fact is general and model independent. Therefore, it should be seen either in a Fermi-liquid or a localized spin model.

The spin-wave excitations predicted by Eq. (26) need not be well defined. A straightforward calculation shows that for $\mathbf{q}=\mathbf{Q}$, the maximum in χ'' occurs at

$$\omega_{\rm max}=\Delta(1-i\gamma), \tag{30}$$

where

$$\gamma=\Delta/\omega_{\rm SF}, \tag{31}$$

from which one obtains

$$\chi''(\mathbf{q},\omega_{\rm max})=\frac{\chi_Q}{\gamma}\,. \tag{32}$$

Hence for a well-defined spin wave ($\gamma\ll 1$), one can find a resonant peak whose magnitude is far in excess of χ_Q, a situation which is to be contrasted with that which one obtains when only relaxational behavior is present, and $\chi''_{\rm max}=\chi_Q/2$. However, as we shall see, in the normal state of the cuprate superconductors, one likely has $\gamma\gtrsim 1$. Indeed, if we use the σ-model result, $c'=0.55c$ in the scaling regime, which extends down to $T_*\lesssim 100$ K in the systems studied in neutron-scattering experiments, then, at (π,π),

$$\gamma=\frac{c}{c'}\simeq 1.8, \quad T_*\lesssim T\lesssim T_{\rm cr}. \tag{33}$$

We note that the relation that we have found above, $\alpha c'=\text{const}$, follows directly from the sum rule for the localized spins,

$$\int d^2q\int d\omega\,\frac{\chi''(\mathbf{q},\omega)}{1-e^{-\omega/T}}\propto\alpha c\propto\alpha c'. \tag{34}$$

As applied to the experimental situation described above, the spin-fermion model provides a reasonable qualitative description of the $z=1$ scaling. Based on our analysis in Sec. III, we have not found signatures of the two crossovers in the scaling regime. From this, together with the results of the measured relaxation rate ratios, which yield $z=1$, we would conclude that within the σ-model multiple spin-wave scattering is the dominant contribution to damping of the spin waves in the underdoped materials. The detailed comparison of this theory with the inelastic neutron-scattering experiments is then obscured by the fact that the correct form of damping for the spin-wave excitations can only be obtained numerically for the experimentally accessible temperature and frequency regions. The "spin pseudogap" temperature in this model is the temperature where scaling stops working; i.e., the effects of the natural distance cutoff ($\sim$ the lattice constant a) are appreciable. It is natural that this happens at certain value of correlation length $\xi_{\rm cr}\simeq 2a$ from Sec. III. Above the temperature $T_{\rm cr}$ scaling analysis becomes inapplicable. It is impossible to obtain the precise value of $T_{\rm cr}$ or $\xi_{\rm cr}$ from the scaling analysis alone. A numerical estimate for $\xi_{\rm cr}$ in the insulator, as mentioned above, is consistent with ours.

B. Nearly antiferromagnetic Fermi liquid description

An alternative approach, the NAFL model,[10] started from the high-doping level, where the magnetic fluctuations have been described as $z=2$ Gaussian.[10] The form Eq. (10) is obtained by a Taylor expansion of the random phase approximation (RPA) susceptibility near the (π,π) point. The characteristic low-energy mode in this model is $\omega_{\rm SF}=\Gamma/\xi^2$, with Γ of the order of Fermi energy. The spin waves are absent, and the spin fluctuations have relaxational character. This model has been successfully applied to the explanation of the relaxation rates in $YBa_2Cu_3O_7$, as discussed in Sec. III.

Recently, Monthoux and Pines[17] (MP) have proposed a phenomenological description of the observed spin pseudogap and $z=1$ scaling behavior which begins at this "other end," the high-doping limit in which a NAFL approach is the appropriate starting point. The NAFL description of magnetic scaling proposed by MP is based on the twin proposal that the strong Coulomb correlations between planar quasiparticles give rise to a second energy scale, $\omega_J\sim$ a few J, and that spin pseudogap behavior is a quasiparticle phenomenon, in which the dynamic irreducible particle-hole susceptibility $\tilde{\chi}(q,\omega)$ for wave vectors in the vicinity of (π,π) becomes temperature dependent for $T\lesssim T_{\rm cr}$. More specifically, MP show that the propagating term in Eq. (26) can arise from the dependence on ω_J of the restoring force $f^a(\mathbf{q},\omega,T)$, which gives rise to NAFL behavior in mean-field theory, in which case the spin gap is related to Δ by

$$\Delta=\omega_J(\tilde{\chi}_Q/\chi_Q)^{1/2}=\omega_J\tilde{\xi}/\xi, \tag{35}$$

where $\tilde{\chi}_Q=\alpha\tilde{\xi}^2$ is the nearly temperature-independent static irreducible particle-hole susceptibility. They also show that if one writes

$$\lim_{\omega\to 0}\tilde{\chi}(Q,\omega)=N_Q(T)\tilde{\chi}_Q\omega, \tag{36}$$

then in the mean-field approximation,

$$\omega_{\rm SF}=\frac{\tilde{\xi}^2}{N_Q(T)\xi^2}\,, \tag{37}$$

where $\tilde{\xi}\simeq\pi^{-1}$. Hence if the "commensurate" quasiparticle density of states, $N_Q(T)$, obeys the relations

$$N_Q(T)=\tilde{\chi}_Q\,,\quad T>T_{\rm cr}\,,\quad N_Q(T)=\frac{\tilde{\xi}^2}{c'}\frac{1}{\xi}=\frac{\tilde{\chi}_Q}{\alpha c'\xi}\,,$$

$$T_*\lesssim T\lesssim T_{\rm cr}\,, \tag{38}$$

then one has the QC $z=1$ scaling behavior $\omega_{\rm SF}=c'/\xi$ for $T_*\lesssim T\lesssim T_{\rm cr}$, while above $T_{\rm cr}$, one recovers nonuniversal mean-field behavior, with $\omega_{\rm SF}\propto\xi^{-2}$.

As MP show, since

$$\frac{^{63}T_1T}{^{63}T_{2G}^2}\propto\chi_Q\omega_{\rm SF}=\tilde{\chi}_Q/N_Q(T) \tag{39}$$

to the extent that $\tilde{\chi}_Q(T)$ is weakly temperature dependent, the temperature dependence of the quantity, $N_Q(T)$, may be directly obtained from experiment. Moreover, on making our ansatz, $\xi_{\rm cr}=2$, then at $T_{\rm cr}$ we have, from Eq. (39), a scaling relation between α and c',

$$\alpha c'=\tfrac{1}{2}, \tag{40}$$

which is quite close to the values determined in Table I. In Fig. 18, we give the results for $T_{2G}^2/(T_1T)$ for $YBa_2Cu_3O_{6.63}$, $YBa_2Cu_4O_8$, and $YBa_2Cu_3O_7$ obtained using Eq. (39) and the experimental results of Takigawa,[8] Imai and Slichter,[35] and Corey *et al.*[36] It is instructive to compare the temperature dependence of $T_{2G}^2/(T_1T)\propto(1/\tilde{\chi}_Q)N_Q(T)$ between T_* and $T_{\rm cr}$ shown in Fig. 18 for the $YBa_2Cu_3O_{6.63}$ and $YBa_2Cu_4O_8$ samples with that found for $\chi_0(T)$, since at long wavelengths one expects to find, by analogy with Eq. (36),

$$\lim_{\omega\to0}\tilde{\chi}''(0,\omega)=N_0(T)\tilde{\chi}_0(T_{\rm cr})\omega$$

$$\simeq\chi_0(T)\tilde{\chi}_0(T_{\rm cr})\omega, \tag{41}$$

with $N_0(T_{\rm cr})\simeq\tilde{\chi}_0(T_{\rm cr})$ and $N_0(T)\propto\chi_0(T)$. We find that $[N_Q(T)/\tilde{\chi}_Q(T)]$ and $\chi_0(T)$ display a comparable temperature variation between T_* and $T_{\rm cr}$; however, although both $[N_Q(T)/\tilde{\chi}_Q]$ and $\chi_0(T)$ vary linearly with T over this temperature region, the respective slopes for the two quantities do not agree.

We further note that the temperature T_* which marks the lower endpoint of magnetic scaling behavior is barely visible in Fig. 18 as the temperature at which $[N_Q(T)/\tilde{\chi}_Q]$ changes slope. From Eq. (39) we see that in the NAFL description of the QD state proposed in MP, at low temperatures, where $\xi\simeq$const, $\omega_{\rm SF}$ varies as $(a+bT)^{-1}$, as is found experimentally, rather than the exponential behavior predicted by the σ model.

V. INELASTIC NEUTRON-SCATTERING RESULTS

In this section we discuss the consistency of the inelastic neutron-scattering experiments with the results of NMR experiments and the scenario developed above. We start with $YBa_2Cu_3O_{6+x}$. Early experiments on this system[42] showed the presence of the gap in the excitations near the antiferromagnetic wave vector, which increased with increasing doping, consistent with the scaling model discussed above. However, it has been difficult to extract the magnetic scattering from the unpolarized neutron experiments due to the presence of acoustic phonons at similar frequencies. The quality of the $YBa_2Cu_3O_{6+x}$ samples and measurements has improved considerably since the early work. In particular, an analysis of magnetic excitations[43,25] has been done in $YBa_2Cu_3O_7$ using a polarized neutron-scattering technique, which enables one to extract the phonon part of the scattering cross section. Detailed experiments[44] have also been performed on the underdoped compound $YBa_2Cu_3O_{6.6}$. In what follows, we focus on these two recent experiments.

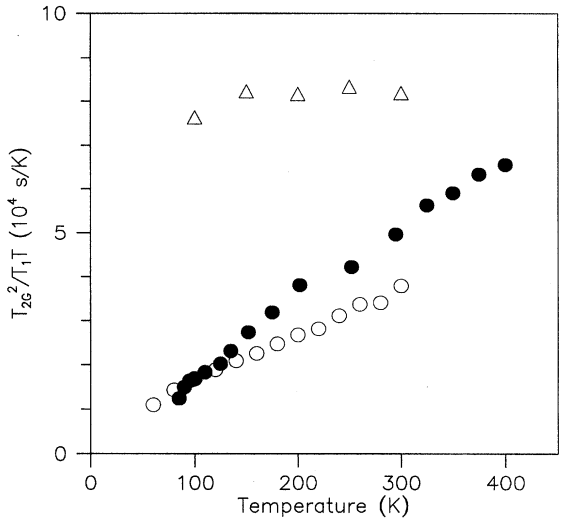

FIG. 18. $^{63}(T_{2G}^2/T_1T)$ ($\propto N_Q(T)/\tilde{\chi}_Q$), extracted from NMR experiments on $YBa_2Cu_3O_{6.63}$, $YBa_2Cu_4O_8$, and $YBa_2Cu_3O_7$.

Fong *at al.*[25] have recently shown experimentally that, contrary to the earlier work of Mook *et al.*,[43] the broad peak at 41 meV corresponding to a magnetic excitation appears *only* in the superconducting state. As a result, they argue that this excitation indeed corresponds to quasiparticle pair creation in the superconducting state. This is a plausible scenario, since Pines and Wrobel[45] find that the superconducting gap, $\Delta=2.6\,k_BT_c$. Here we wish to suggest an alternative explanation for the 41 meV magnetic peak: *that it is a spin wave which only becomes visible as a distinct excitation in the superconducting state.* Such an excitation is consistent with the singlet to triplet transition identified by Fong *et al.*[25] As we have remarked in Sec. IV, the spin-wave excitation is overdamped in the normal state. It is much better defined in the superconducting state, because NMR experiments show that $\omega_{\rm SF}$ increases rapidly for $T<T_c$; indeed, for $YBa_2Cu_3O_7$, Martindale *et al.*[46] find, $\omega_{\rm SF}(0.75T_c)\simeq\omega_{\rm SF}(T_c)/10$. As a result, the gap in the spin excitation spectrum, $\Delta=c/\xi$, should be observable in inelastic neutron-scattering experiments. From our analysis for $YBa_2Cu_3O_7$ we obtain $c'\simeq35$ meV and $\xi(T_c)\simeq2.3$. If $\Delta\sim41$ meV, then one must have

$$c=\Delta\xi\sim 90 \text{ meV}. \tag{42}$$

As a result, in the normal state, $\gamma=\Delta/\omega_{SF}\simeq 2.5$, and the spin-wave excitations would be unobservable there, in agreement with the conclusion of Fong *et al.*.[25] On the other hand, at $T\simeq 0.75T_c$, one has $\gamma\simeq 0.25$, and the excitation becomes readily observable.

We next consider the σ model and NAFL interpretation of this result. In the σ model, if the damping of spin excitations is accounted by multiple spin scattering *alone*, the gap in the spectrum of magnetic excitations would be $\Delta(T_c)\simeq 28$ meV. Since the actual gap is considerably larger, the fermionic source of damping must be appreciable in $YBa_2Cu_3O_7$. Using $\Delta=1.82\omega_{spin}\xi$ and Eq. (27), we obtain $\omega_{spin}/\omega_{fermion}\simeq 0.47$ as the ratio of the fermionic and spin sources of damping. Thus, the spin excitation in $YBa_2Cu_3O_7$ could be a spin wave. As the temperature decreases below T_c the particle-hole damping disappears. The gap in the spin-wave spectrum causes the "spin" part of damping to also decrease with temperature. As a result, the spin-wave spectrum is much better defined in the superconducting state.

In the NAFL description,

$$c=\omega_J\tilde{\xi}, \tag{43}$$

so that $\omega_J\sim 2J$, a not unreasonable value, while ω_{SF} of course reflects only quasiparticle behavior, with its rapid increase below T_c being *entirely* a consequence of the superconducting gap. Moreover, measurements of T_{2G}^{-1} in the superconducting state of $YBa_2Cu_3O_8$ (Ref. 36) show that it gradually decreases below T_c, a decrease which, according to Eq. (13), directly reflects a decrease in ξ. Since $\Delta=c/\xi$, we would accordingly expect a corresponding increase in Δ. There are at present no measurements of T_{2G} for $YBa_2Cu_3O_7$; if we assume that ξ decreases, by some 20%, from 2.2 at T_c to 1.8 for $T\lesssim T_c/2$ (by which temperature the gap is fully established), then a value of ~ 1.9 at $0.75T_c$ is not unreasonable. On taking $c=74$ meV, we would then find $\Delta=39$ meV at 70 K and $\Delta\simeq 41$ meV for $T\lesssim 0.5T_c$, a result in reasonable agreement with experiment.

We next estimate the spin-wave spectrum in $YBa_2Cu_3O_{6.55}$, where detailed inelastic neutron-scattering results were reported recently by Sternlieb *et al.*[44] From our analysis we find $c'\simeq 70$ meV. In the σ model, the "spin" source of damping may be expected to be dominant for this compound, and therefore $c\simeq 127$ meV. Since this compound is close to the insulator metal border, and exact doping level is not known, the correlation length is hard to determine by extrapolation. To obtain a gap of $\Delta\simeq 10$ meV, which is experimentally observed, we need $\xi\simeq 12.7$ at low temperature, a value which would require that the system be at a lower doping level than $YBa_2Cu_3O_{6.63}$. In the NAFL description, c would not be expected to change appreciably with doping, so that with $c=74$ meV, we find a low-temperature gap of 10 meV with $\xi=7.4$. This latter length is just what we find for $YBa_2Cu_3O_{6.63}$ near T_c, and so the NAFL description is clearly consistent with the emergence of a spin gap at 10 meV well below T_c.

Sternlieb *et al.* found that the local (integrated) spin susceptibility $\chi_L''(\omega)$ exhibits ω/T scaling. The temperature at which the scaling breaks down decreases with increasing ω. This scaling behavior is generic for the $z=1$ QC regime. The scaling function for $\chi_L''(\omega/T)$ was found by Chubukov and Sachdev.[6] In the region of ω and T where the magnetic response was measured, $\chi''(\omega/T)\propto\omega/T$, consistent with experiment. The decrease of the temperature T_* with increasing energy transfer is also expected on the basis of scaling arguments.

Provided γ is small enough, the spin-wave spectrum that we predict can be observed in neutron-scattering experiments. According to Eq. (26), for $\omega>\Delta$, $\chi''(\mathbf{q},\omega)$ is peaked at the incommensurate wave vector, displaced from (π,π) by $\delta q=\sqrt{\omega^2-\Delta^2}/c$. However, direct measurement of the spin-wave spectrum in $YBa_2Cu_3O_{6.6}$ is obscured by some relatively large degree of imcommensuration observed in this material.[47] We estimate the width enhancement due to the spin waves at 30 meV for this material as $2\delta q\simeq 0.05$ radiation length units (r.l.u.) while the experimental width of the peak is $\sim 0.25\pm 0.1$ r.l.u. is independent of energy transfer. Thus the predicted peak width enhancement agrees within experimental error with the value reported by Sternlieb *et al.*[44]

We now consider $La_{1.85}Sr_{0.15}CuO_4$, a compound where an extensive neutron-scattering study[48] of magnetic excitations has been reported. We note first that the magnetic excitations were found at incommensurate positions, in contradiction with the one-component theory of NMR discussed in Sec. II, which requires that $\chi''(\mathbf{q},\omega)$ be peaked at a commensurate wave vector. According to Barzykin *et al.*,[49] the only possible resolution of this contradiction in the framework of the one-component model lies in the assumption of some sort of domain formation due to tiny regions of phase separation. If this is not what happens, more than one copper spin component should be involved. We further assume that the one-component theory is correct, and imply the presence of some internal superstructure leading to four distinct peaks in the neutron-scattering experiment. However, we note that the analysis done here is more general than the one-component theory reviewed in Sec. II, since it is based on copper NMR only, and the possible incommensurability is not terribly important. Since $^{63}T_{2G}$ experimental results are not so far available, to our knowledge, in the metallic $La_{1.85}Sr_{0.15}CuO_4$, it is not possible to determine all the parameters entering theory. We find that for $\alpha=15$ states/eV, $c'\simeq 29$ meV, and $\xi\simeq 7$. Thus, this leads to a predicted spin gap, $\Delta\simeq 7.5$ meV, for the σ model, and $\Delta\simeq 10$ meV if $c=74$ meV for this compound. We also predict $z=1$ scaling for $T>90$ K. This temperature T_* should decrease with increasing energy transfer. None of these effects have been so far observed in $La_{1.85}Sr_{0.15}CuO_4$. We found some vague indication of the spin gap of ~ 6 meV in the integrated intensity measurements at 35 K, where the most detailed experimental study was reported. However, further study at higher temperatures is required, in which the kind of scaling plot for the integrated intensity such as the one used by Sternlieb *et al.* in $YBa_2Cu_3O_{6.6}$ would be extremely useful. We note that $z=1$ scaling was found by Keimer *et al.*[50] in 2:1:4 system at lower doping level, in the insulating state, as expected from the model discussed above.

The determination made here of the spin fluctuation parameters α and ξ for the 1-2-3 system enables us to estimate the maximum spin fluctuation signal strength $\sim\chi_Q/2$, measurable in inelastic neutron-scattering experiments on the normal state. We find that χ_Q ranges from 69 states/eV for $YBa_2Cu_3O_7$ to 470 states/eV for $YBa_2Cu_3O_{6.63}$; this provides a partial explanation of the difficulty (compared to $O_{6.63}$) in carrying out quantitative measurements on the fully doped members of this family. As we have noted above, in the supercondicting state, once quasiparticle excitations can no longer damp the spin gap excitation at Δ, a considerably shorter signal $\sim(\chi_Q/\gamma)$, where $\gamma\lesssim 1/3$, emerges from the continuum. We can carry out a complete estimate for χ_Q for the 2:1:4 system if we assume that for this system as one finds a result similar to that found for the 1:2:3 system, $c'\alpha\sim 0.54$. We then find, through interpolation between our results for the $Sr_{0.13}$ and $Sr_{0.15}$ samples, that $\chi_Q\sim 790$ states/eV for $La_{1.86}Sr_{0.14}CuO_4$ and $\chi_Q\sim 2400$ states/eV for $La_{1.9}Sr_{0.1}CuO_4$. Thus one can anticipate significantly stronger spin fluctuation signals in the 2:1:4 system. It is interesting to note that the value of the correlation length at T_* for $La_{1.86}Sr_{0.14}CuO_4$ is $\xi\sim 8$, comparable to that found by Mason *et al.*[48] in their neutron-scattering experiments on this system.

We do not attempt to compare, in this paper, the correlation length obtained in our analysis of the NMR experiments in $YBa_2Cu_3O_{6+x}$ system with that measured in the inelastic neutron-scattering experiments. Part of the reason is that the observed peak at the commensurate wave vector is very broad, a result which would lead to an oxygen NMR spin-lattice relaxation rate which is in disagreement with experiment. On the other hand, the neutron-scattering experiments of Tranquada *et al.*[47] in $YBa_2Cu_3O_{6.6}$ have suggested the presence of an unresolved four-peak superstructure. This superstructure, if present, would make such a comparison meaningless.

VI. CONCLUSION

The "spin pseudogap" effect in the cuprate superconductors is a puzzling phenomenon which corresponds to a reduction of the effective density of states. We show that this effect is present, and has similar character, in both single-plane $La_{2-x}Sr_xCuO_4$ and in bilayer $YBa_2Cu_3O_{6+x}$ families. As a result, we have pursued a single-plane scenario for this effect in which any coupling between the bilayers does not play a crucial role. We find in this scenario that the development of the "spin pseudogap" corresponds to the onset of scaling at a certain value of correlation length. The value of the dynamical critical exponent in the scaling regime is $z=1$.

We have analyzed a large collection of experiments using the scaling theory (the QNLσ model) and the NAFL approach. The scaling theory is based on the existence of spin-wave excitations in the metallic cuprates, which have a finite energy gap at (π,π) and a linear dispersion law at high frequency. It should be emphasized that there is no gap other than the gap of the spin-wave excitations in the σ model. This gap should be observable in inelastic neutron-scattering experiments in the superconducting state, and may have been seen as the 41 meV excitation in $YBa_2Cu_3O_7$. The "spin pseudogap" observed in the bulk magnetic susceptibility or specific heat measurements is of different character; it *does not necessarily correspond* to a gap in the quasiparticle spectrum. We relate the observed spin pseudogap behavior to the onset of scaling behavior at high temperatures. It should be noted that a scenario in which the spin pseudogap phenomenon is related to a failed spin-density-wave (SDW) gap[51] is also possible. This mechanism is somewhat similar to the NAFL framework, considered in Sec. IV, in which novel physics arises if one takes into account vertex corrections brought about by stroing magnetic correlations.

In summary, we have applied the $z=1$ nearly antiferromagnetic Fermi-liquid scaling theory to the analysis of the bulk susceptibility, NMR $^{63}T_1$ and $^{63}T_{2G}$ relaxation rates, specific heat, resistivity, Hall effect, and inelastic neutron-scattering experiments in the $La_{2-x}Sr_xCuO_4$ and $YBa_2Cu_3O_{6+x}$ families. The magnetic phase diagrams for the two compounds display the same behavior, and can be superposed on one another, when plotted as a function of hole concentration. Two magnetic crossovers are evident from experimental data. The upper crossover, at T_{cr}, corresponds to the onset of the $z=1$ scaling behavior. We argue that above T_{cr} the spin dynamics is nonuniversal, i.e., influenced by the lattice cutoff. As a result, no definite predictions can be made on the basis of scaling theory for $T>T_{cr}$. Below T_{cr} scaling applies, and universal scaling functions can be computed. The temperature T_{cr} decreases with increasing doping. The lower crossover temperature, T_* marks the low-temperature end of the $z=1$ quantum critical scaling behavior, and its appearance is predicted by the scaling theory. The magnetic susceptibility, the NMR relaxation rates $^{63}T_1T$, $^{63}T_{2G}$, and the resistivity are linear in the quantum critical regime between T_* and T_{cr}. Both crossovers disappear in the overdoped case, as the correlation length becomes too short for $z=1$ scaling to apply. These considerations are summarized on Figs. 2, 3. There is no region of applicability for $z=2$ Fermi-liquid scaling on our magnetic phase diagram in the normal state. The observed ratio $^{63}T_1T/^{63}T_{2G}^2=$const in $YBa_2Cu_3O_7$, in our interpretation, corresponds to a mean-field nonuniversal behavior.

On making the ansatz that $\xi_{cr}=2$ at the critical temperature T_{cr} which marks the onset of the $z=1$ QC regime, we have determined, from the NMR experiments, the correlation length as a function of temperature for both $YBa_2Cu_3O_{6+x}$ and $La_{2-x}Sr_xCuO_4$ families, and the spin-wave velocity in $YBa_2Cu_3O_{6+x}$ as a function of doping. From this analysis, we can approximately obtain the energy spectrum of the spin waves, which should be observed in inelastic neutron-scattering experiments on the superconducting state. Thus, in our scenario, the peak in magnetic inelastic neutron scattering in $YBa_2Cu_3O_7$ at 41 meV, and the spin gap of 10 meV observed in $YBa_2Cu_3O_{6.6}$ could originate in spin waves. The observation of the full spin-wave spectrum is obscured in these materials by strong phonon scattering and by some degree of discommensuration found in $YBa_2Cu_3O_{6.6}$.

In arriving at our magnetic phase diagram, we have frequently had to resort to interpolation and extrapolation from existing experimental data. Our calculations are, in many cases, directly subject to experimental test. It is our hope and expectation that the NMR experimental community will now fill in the interstices, and so make more precise the depen-

dence of T_{cr} and T_* on hole concentration. For example, detailed measurements of $^{63}T_{cr}$, $^{63}T_1$, and $\chi_0(T)$ carried out on the same samples, for samples of known oxygen concentration in the vicinity of $YBa_2Cu_3O_{6.95}$, cannot only determine T_{cr} in this region, and establish its dependence on hole concentration, but can also verify whether, as we have conjectured, the ratio $^{63}T_1T/^{63}T_{2G}$ becomes independent of temperature below T_{cr}. In a similar vein more detailed measurements on the Knight shift and $^{63}T_1$ of the overdoped 2:1:4 system will help one to deduce T_* and T_{cr} for this system.

ACKNOWLEDGMENTS

We are especially grateful to Takashi Imai, Charlie Slichter, and Bob Corey for communicating their data prior to publication and for numerous discussions of the above topics. We also thank L. P. Gor'kov, A. J. Millis, J. R. Schrieffer, Q. Si, A. Sokol, B. Stojkovic, and Y. Zha for the discussions of these and related subjects. This work was supported by NSF Grant No. DMR91-20000 through the Science and Technology Center for Superconductivity.

[1] For recent reviews, see C. P. Slichter, in *Strongly Correlated Electron Systems*, edited by K. S. Bedell *et al.* (Addison-Wesley, Reading, MA, 1994), p. 427; and D. Pines, in *High Temperature Superconductors and the C-60 system*, edited by T. D. Lee and H. C. Ren (Gordon and Breach, New York, in press).

[2] E. Manousakis, Rev. Mod. Phys. **63**, 1 (1991).

[3] S. Chakravarty, B. I. Halperin, and D. R. Nelson, Phys. Rev. B **39**, 2344 (1989).

[4] P. W. Anderson, Science **235**, 1196 (1987).

[5] S. Sachdev and J. Ye, Phys. Rev. Lett. **69**, 2411 (1992).

[6] A. V. Chubukov and S. Sachdev, Phys. Rev. Lett. **71**, 169 (1993); A.V. Chubukov, S. Sachdev, and J. Ye, Phys. Rev. B **49**, 11 919 (1994).

[7] T. Imai *et al.*, Phys. Rev. Lett. **70**, 1002 (1993).

[8] M. Takigawa, Phys. Rev. B **49**, 4158 (1994).

[9] A. Sokol and D. Pines, Phys. Rev. Lett., **71**, 2813 (1993).

[10] A. Millis, H. Monien, and D. Pines, Phys. Rev. B **42**, 167 (1990).

[11] K. Ueda, T. Moriya, and Y. Takahashi, J. Phys. Chem. Solids **53**, 1515 (1992); T. Moriya, Y. Takahashi, and K. Ueda, J. Phys. Soc. Jpn. **59**, 2905 (1990).

[12] D. Thelen, D. Pines, and J.-P. Lu, Phys. Rev. B **47**, 9151 (1993).

[13] V. Barzykin, D. Pines, A. Sokol, and D. Thelen, Phys. Rev. B **49**, 1554 (1994).

[14] S. Sachdev, A. V. Chubukov, and A. Sokol, Phys. Rev. B **51**, 14 874 (1995).

[15] A. J. Millis, Phys. Rev. B **48**, 7183 (1993).

[16] B. L. Altshuler, L. B. Ioffe, A. I. Larkin, and A. J. Millis, Phys. Rev. B **52**, 4607 (1995).

[17] P. Monthoux and D. Pines, Phys. Rev. B **50**, 16 015 (1994).

[18] D. C. Johnston, Phys. Rev. Lett. **62**, 957 (1989).

[19] H. Alloul *et al.*, Phys. Rev. Lett. **63**, 1700 (1989).

[20] J. Loram *et al.*, Phys. Rev. Lett. **71**, 1740 (1993); J. Supercond. **7**, 243 (1994).

[21] T. Ito, K. Takenako, and S. Uchida, Phys. Rev. Lett. **70**, 3995 (1993).

[22] B. Bucher *et al.*, Phys. Rev. Lett. **70**, 2012 (1993).

[23] H. Y. Hwang *et al.*, Phys. Rev. Lett. **72**, 2636 (1994).

[24] T. Nakano *et al.*, Phys. Rev. B **49**, 16 000 (1994).

[25] H. F. Fong, B. Keimer, P W. Anderson, D. Reznik, F. Dogan, and I. A. Aksay, Phys. Rev. Lett. **75**, 316 (1995).

[26] M. Takigawa *et al.*, Phys. Rev. B **43**, 247 (1991).

[27] B. Shastry, Phys. Rev. Lett. **63**, 1288 (1989); F. Mila and T. M. Rice, Physica C **157**, 561 (1989).

[28] D. Thelen and D. Pines, Phys. Rev. B **49**, 3528 (1994).

[29] H. Monien, D. Pines, and M. Takigawa, Phys. Rev. B **43**, 258 (1991).

[30] A. J. Millis and H. Monien, Phys. Rev. Lett. **70**, 2810 (1993); Phys. Rev. B **50**, 16 606 (1994).

[31] S. Ohsugi *et al.*, J. Phys. Soc. Jpn. **63**, 700 (1994).

[32] N. Elstner, R. L. Glenister, R. R. P. Singh, and A. Sokol, Phys. Rev. B **51**, 8984 (1995).

[33] A. P. Reyes *et al.*, Phys. Rev. B **43**, 2989 (1991).

[34] R. E. Walstedt *et al.*, Phys. Rev. B **45**, 8074 (1992).

[35] T. Imai and C. P. Slichter, Phys. Rev. B **47**, 9158 (1993).

[36] R. Corey, N. Curro, T. Imai, K. O'Hara, C. P. Slichter, and H. Kosuge (private communication).

[37] H. Zimmerman, Physica C **185-189**, 1145 (1991).

[38] Y.-L. Liu and Z.-B. Su, Phys. Lett. A **200**, 393 (1995).

[39] V. J. Emery, Phys. Rev. Lett. **58**, 2794 (1987); L. P. Gor'kov, V. N. Nicopoulos, and P. Kumar, J. Supercond. **7**, 505 (1994), and references therein.

[40] M. Lindroos *et al.*, Physica C **212**, 347 (1993).

[41] Lev P. Gor'kov (private communication).

[42] J. Rossat-Mignod *et al.*, Phys. Scr. **T45**, 74 (1992); J. Rossat-Mignod *et al.*, Physica B **180&181**, 383 (1992), and references therein.

[43] H. Mook *et al.*, Phys. Rev. Lett. **70**, 3490 (1993).

[44] B. J. Sternlieb *et al.*, Phys. Rev. B **47**, 5320 (1993).

[45] D. Pines and P. Wrobel (unpublished).

[46] J. Martindale *et al.*, Phys. Rev. B **47**, 9155 (1993).

[47] J. M. Tranquada *et al.*, Phys. Rev. B **46**, 5561 (1992).

[48] S.-W. Cheong *et al.*, Phys. Rev. Lett. **67**, 1791 (1991); T.E. Mason, G. Aeppli, and H.A. Mook, *ibid.* **68**, 1414 (1992); G. Aeppli and T.E. Mason (private communication).

[49] V. Barzykin, D. Pines, and D. Thelen, Phys. Rev. B **50**, 16 052 (1994).

[50] B. Keimer *et al.*, Phys. Rev. Lett. **67**, 1930 (1991).

[51] A. P. Kampf and J. R. Schrieffer, Phys. Rev. B **41**, 6399 (1990); **42**, 7967 (1990).